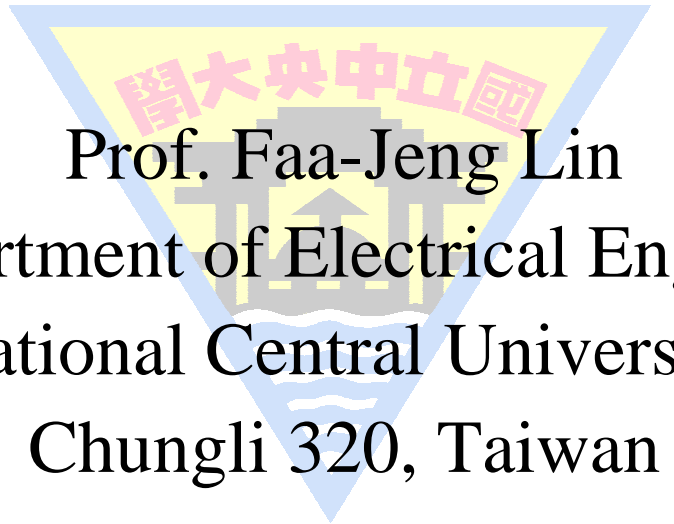




Development of Intelligent Control Systems for Linear Motor Drives



Prof. Faa-Jeng Lin
Department of Electrical Engineering
National Central University
Chungli 320, Taiwan
E-mail: linfj@ee.ncu.edu.tw

- **Linear Induction Motor (LIM) Drive**

F. J. Lin et al., “Hybrid control using recurrent-fuzzy-neural-network for linear induction motor servo drive,” *IEEE Trans. Fuzzy Systems*, vol. 9, no. 1, pp. 1-15, 2001.

- **Linear Synchronous Motor (LSM) Drive**

F. J. Lin et al., “Hybrid supervisory control using recurrent fuzzy neural network controller for tracking periodic inputs,” *IEEE Trans. Neural Network*, vol. 12, no. 1, pp. 68-90, 2001.

- **Piezo Ceramic Linear Ultrasonic Motor (LUSM) Drive**

F. J. Lin et al., “Recurrent fuzzy neural network control for piezoelectric ceramic linear ultrasonic motor drive,” *IEEE Tran. Ultra. Ferro. Freq. Ctrl.*, vol. 48, no. 4, 2001.

- **X-Y Table Based on Permanent Magnet Linear Synchronous Motor (PMLSM)**

F. J. Lin et al., “Robust Fuzzy-Neural-Network Sliding-Mode Control for Two-Axis Motion Control System,” *IEEE Tran. Industrial Electronics*, vol. 53, no. 4, 2006.
(SCI)

I. Linear Induction Motor Drive

- LIM has many excellent features such as high-starting thrust force, alleviation of gear between motor and the motion devices, reduction of mechanical losses and the size of motion devices, high-speed operation, silence, etc.
- An experimental LIM is shown in Fig. 1.



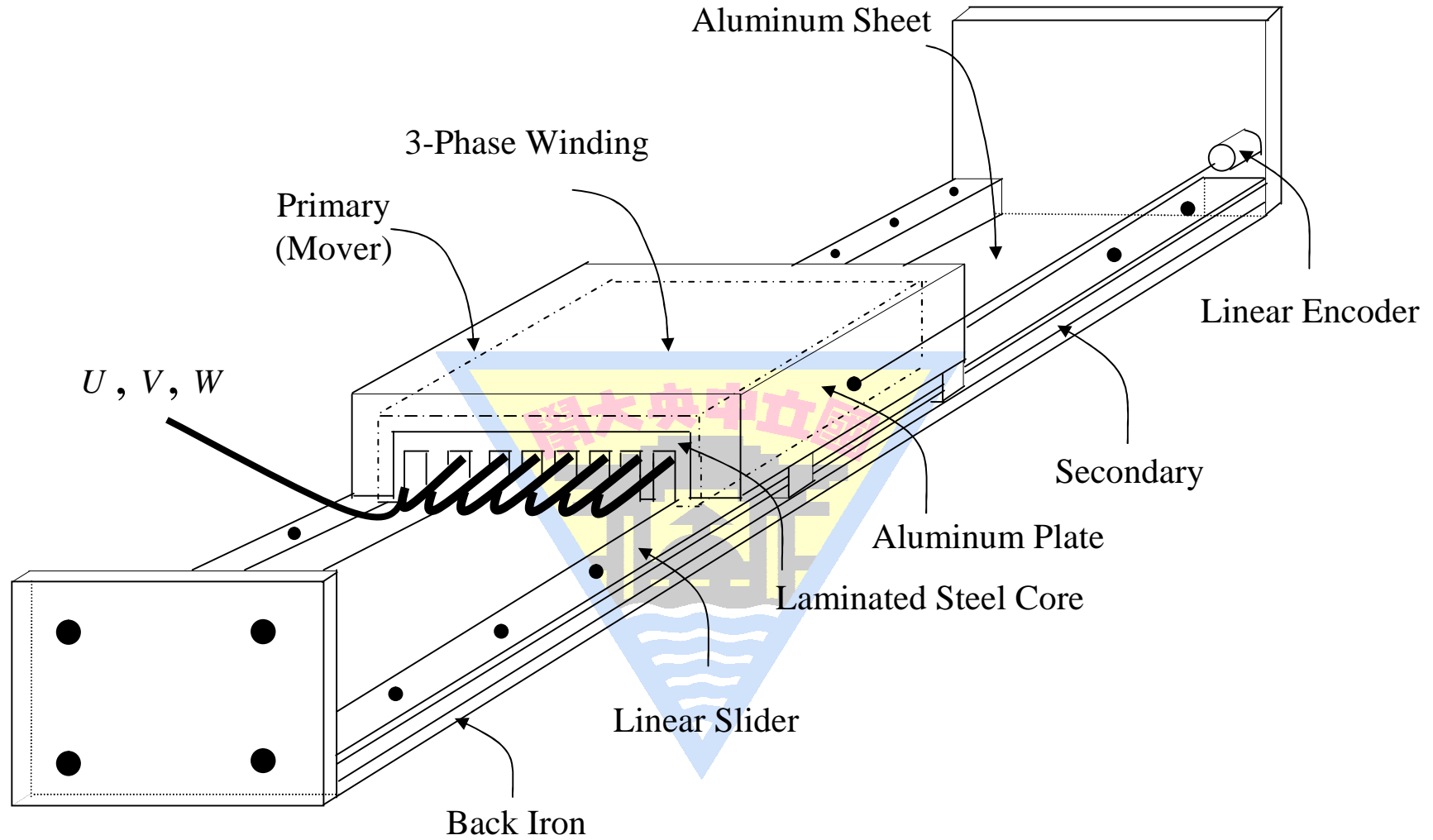


Fig. 1

- LIM has been widely used in the field of industrial processes and transportation applications.
- Motor parameters are time varying due to the change of operating conditions, such as speed of mover, temperature and configuration of rail. Furthermore, LIM is greatly affected by force ripple and external disturbances because there is no auxiliary mechanisms such as gears or ball screws equipped.
- Decoupled control approaches, such as field-oriented control and nonlinear state feedback techniques, have been widely used in the design of induction motor drives for high-performance applications.

- Nonlinear state feedback control utilizes the feedback linearization approach can achieve input-output decoupling control and good dynamic performance for induction motors. With the input-output linearization approach and the adaptive flux observer, the decoupled control of the LIM is guaranteed.
- Control performance of the LIM is still influenced by the uncertainties of the plant. A suitable control scheme is designed to confront the uncertainties existed in practical applications of the LIM.

- A block diagram of the nonlinear decoupled LIM servo drive system combined with an adaptive flux observer is shown in Fig. 2, which consists of a ramp-comparison current-controlled pulse width modulated (PWM) voltage source inverter (VSI), a feedback linearization controller, two coordinate translators, a speed-control loop, and a position-control loop. The LIM used in this drive system is a three-phase Y-connected two-pole 3kW 60Hz 180V/14.2A type.

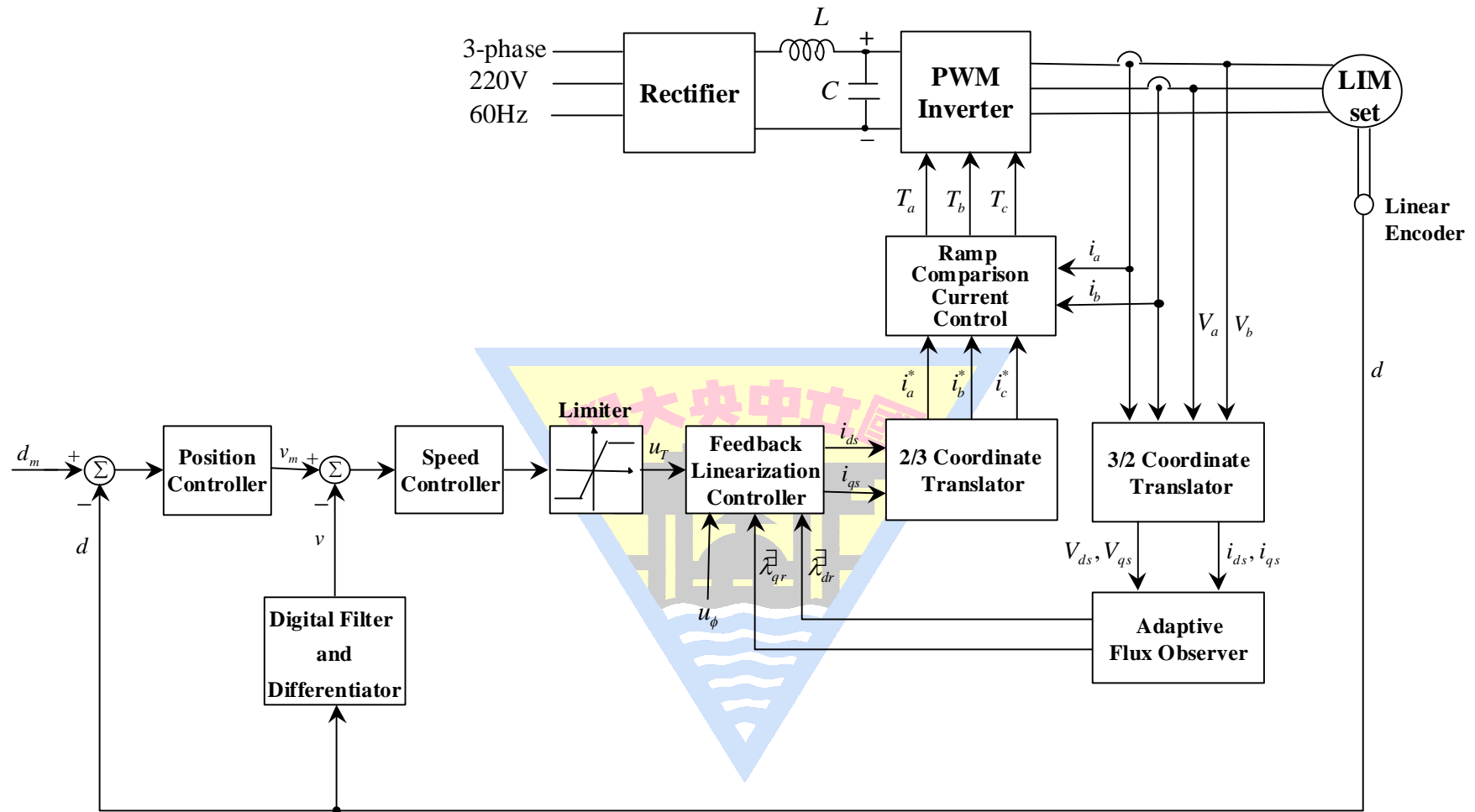


Fig. 2

- Dynamic model of the LIM in d - q stationary reference frame:

$$\dot{i}_{qs} = -\left(\frac{R_s}{\sigma L_s} + \frac{1-\sigma}{\sigma T_r}\right) i_{qs} - \frac{n_p L_m \pi}{\sigma L_s L_r h} v \lambda_{dr} + \frac{L_m}{\sigma L_s L_r T_r} \lambda_{qr} + \frac{1}{\sigma L_s} V_{qs} \quad (1)$$

$$\dot{i}_{ds} = -\left(\frac{R_s}{\sigma L_s} + \frac{1-\sigma}{\sigma T_r}\right) i_{ds} + \frac{L_m}{\sigma L_s L_r T_r} \lambda_{dr} + \frac{n_p L_m \pi}{\sigma L_s L_r h} v \lambda_{qr} + \frac{1}{\sigma L_s} V_{ds} \quad (2)$$

$$\dot{\lambda}_{qr} = \frac{L_m}{T_r} i_{qs} + n_p \frac{\pi}{h} v \lambda_{dr} - \frac{1}{T_r} \lambda_{qr} \quad (3)$$

$$\dot{\lambda}_{dr} = \frac{L_m}{T_r} i_{ds} - \frac{1}{T_r} \lambda_{dr} - n_p \frac{\pi}{h} v \lambda_{qr} \quad (4)$$

$$F_e = K_f (\lambda_{dr} i_{qs} - \lambda_{qr} i_{ds}) = M \dot{v} + Dv + F_L \quad (5)$$

where $T_r = L_r / R_r$, $\sigma = 1 - (L_m^2 / L_s L_r)$, $K_f = 3n_p \pi L_m / (2hL_r)$

- Amplitude of secondary flux is as follows:

$$\lambda_r = \sqrt{(\lambda_{dr})^2 + (\lambda_{qr})^2} \quad (6)$$

- Use (3) and (4), then:

$$\dot{\lambda}_r = -\frac{\lambda_r}{T_r} + \frac{L_m (i_{ds} \lambda_{dr} + i_{qs} \lambda_{qr})}{T_r \lambda_r} \quad (7)$$

From (5), the LIM motion dynamics can be expressed as

$$\dot{v} = -\frac{D}{M} v + \frac{K_f}{M} (\lambda_{dr} i_{qs} - \lambda_{qr} i_{ds}) - \frac{F_L}{M} \quad (8)$$

i_{ds} and i_{qs} are the control inputs, and λ_r and v are the system outputs. Thus, the LIM dynamic is a coupled system.

- Nonlinear state feedback theory is used to eliminate this coupling relationship. Two new control inputs are chosen as follows:

$$\begin{bmatrix} u_\phi \\ u_T \end{bmatrix} = \frac{1}{\lambda_r} \begin{bmatrix} \lambda_{dr} & \lambda_{qr} \\ -\lambda_r \lambda_{qr} & \lambda_r \lambda_{dr} \end{bmatrix} \begin{bmatrix} i_{ds} \\ i_{qs} \end{bmatrix} \quad (9)$$

From (9), the feedback linearization controller can be derived as follows:

$$\begin{bmatrix} i_{ds} \\ i_{qs} \end{bmatrix} = \frac{1}{\lambda_r^2} \begin{bmatrix} \lambda_r \lambda_{dr} & -\lambda_{qr} \\ \lambda_r \lambda_{qr} & \lambda_{dr} \end{bmatrix} \begin{bmatrix} u_\phi \\ u_T \end{bmatrix} \quad (10)$$

- Substituting (10) into (7) and (8), the decoupled equations can be obtained as follows:

$$\dot{\lambda}_r = -\frac{\lambda_r}{T_r} + \frac{L_m u_\phi}{T_r} \quad (11)$$

$$\dot{v} = -\frac{D}{M} v + \frac{K_f}{M} u_T - \frac{F_L}{M} \quad (12)$$

- By using the nonlinear decoupled technique, the electromagnetic force can be represented by

$$F_e = K_f u_T \quad (13)$$

- A hybrid control system shown in Fig. 3 is proposed to control the mover of the LIM for periodic motion. The recurrent-fuzzy-neural-network (RFNN) controller shown in Fig. 4 is the main tracking controller, which is used to mimic a perfect control law, and the compensated controller is proposed to compensate the difference between the perfect control law and the RFNN controller.
- RFNN has the merits of fuzzy inference, dynamic mapping and fast convergence speed. An on-line parameter training methodology, which is derived using the Lyapunov stability theorem and the gradient descent method, is proposed to increase the learning capability of the RFNN.

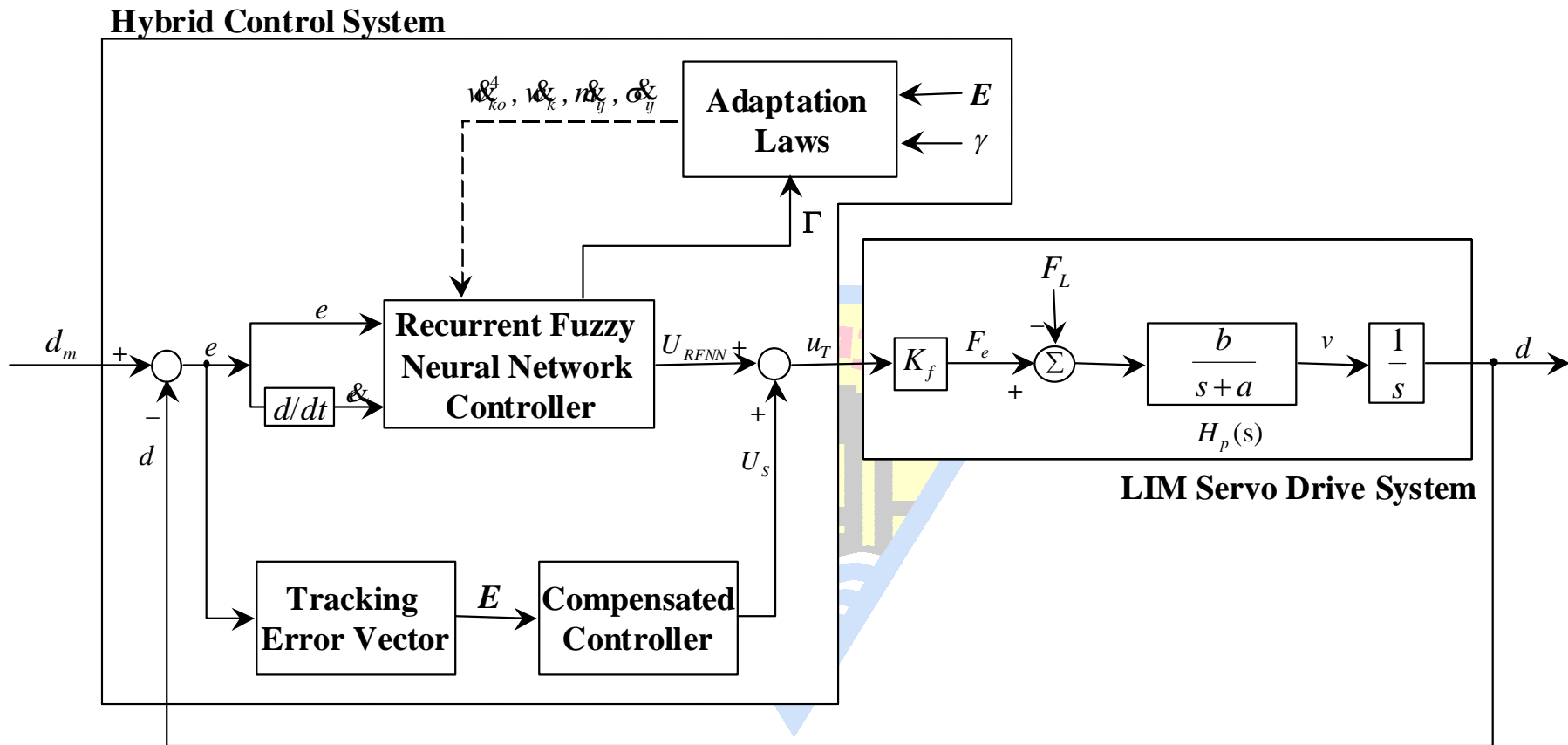


Fig. 3

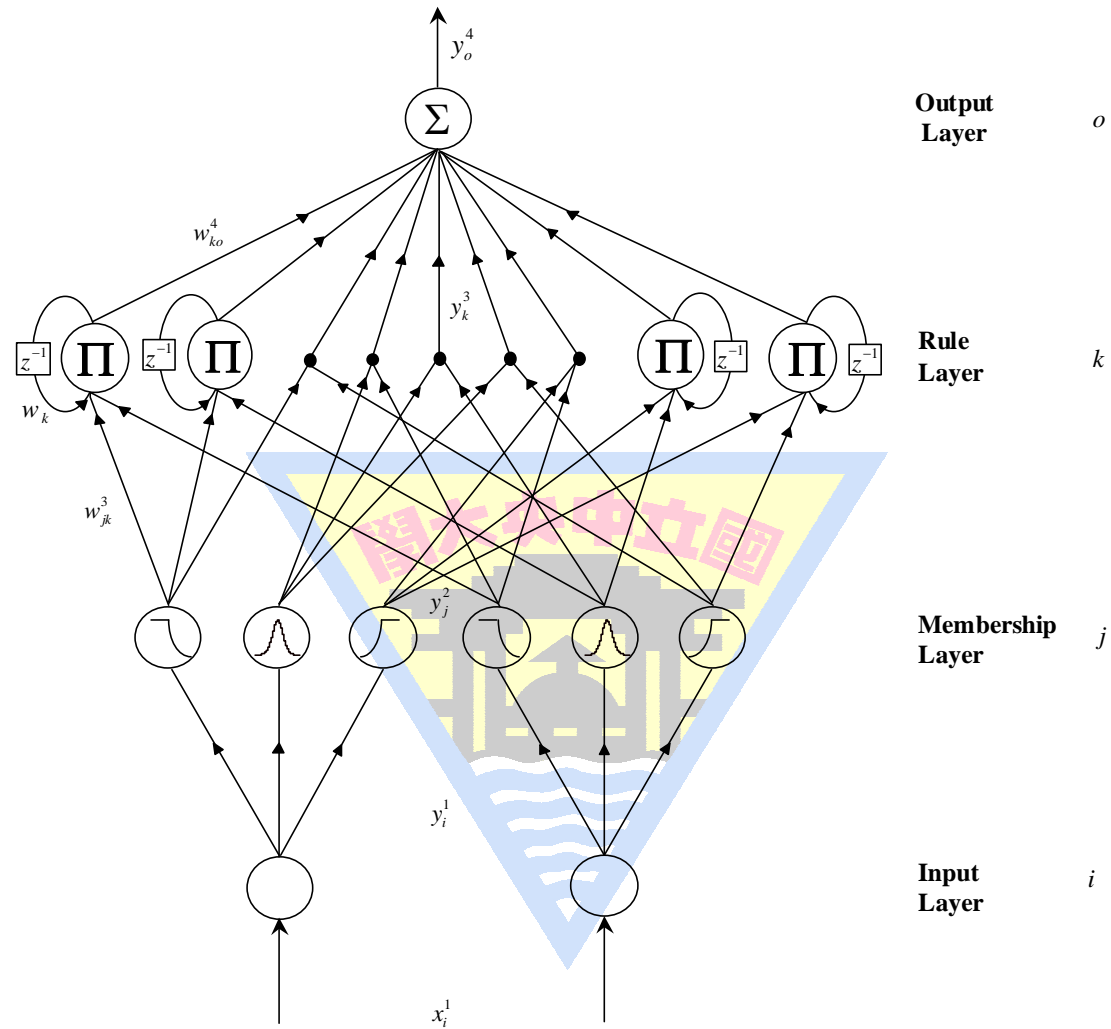


Fig. 4

- A block diagram of the DSP-based computer control system for a LIM servo drive using the current-controlled technique is shown in Fig. 5. The current-controlled PWM VSI is implemented by an IPM switching component with a switching frequency of 15kHz. A servo control card is installed in the control computer. The resulting precision is one pulse to $50\mu\text{m}$.

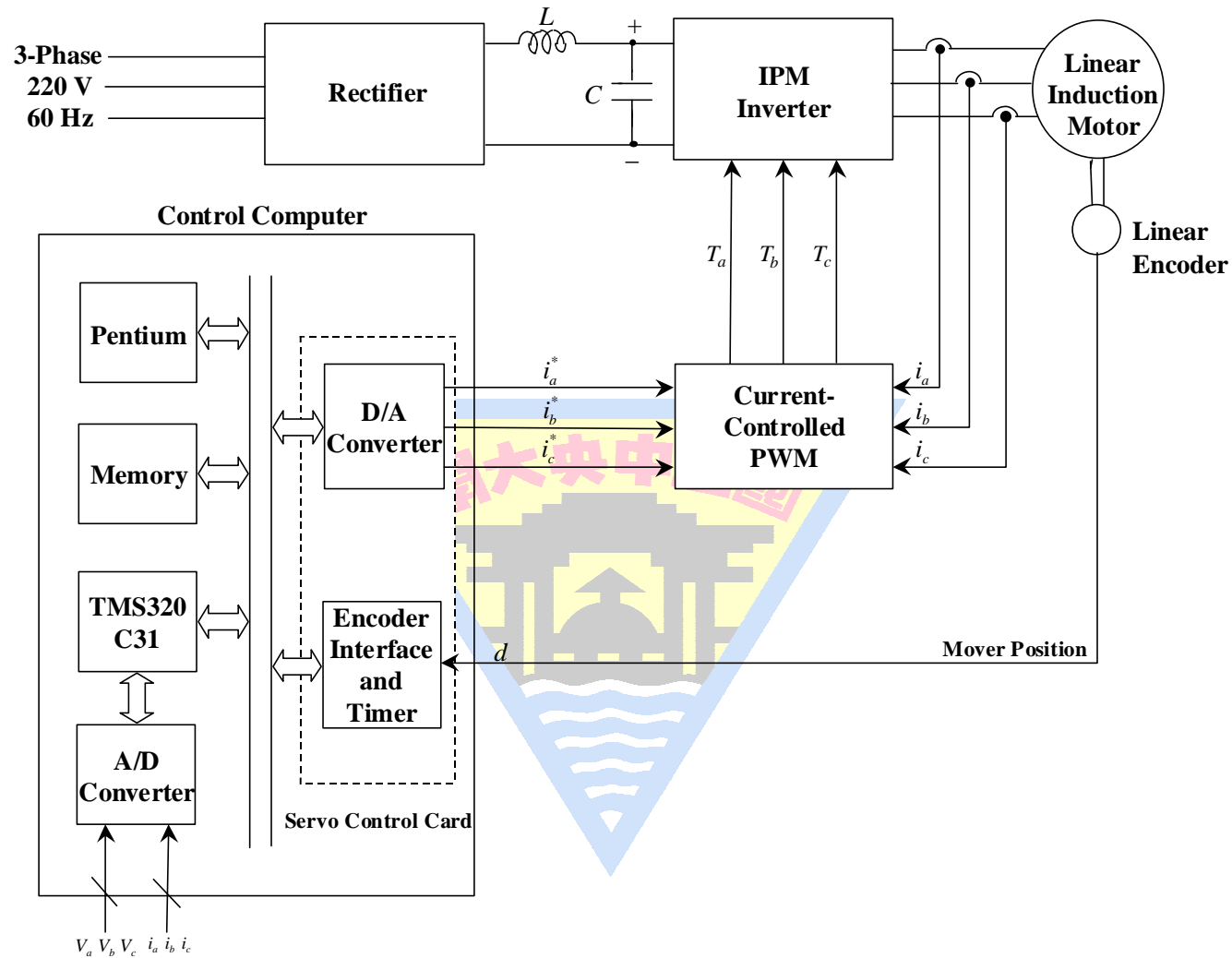


Fig. 5

- The feedback linearization controller and the hybrid control system are realized in a Pentium CPU. The adaptive flux observer is realized in a TMS320C31 DSP. The control intervals of the feedback linearization controller and the observation system are set at 0.2msec, and the control interval of the position control loop is set at 1msec. The control objective is to control the mover to move 0.1m to -0.1m periodically.
- Experimental results of the hybrid control system due to periodic sinusoidal command at the nominal case and the parameter variation case are shown in Fig. 6.

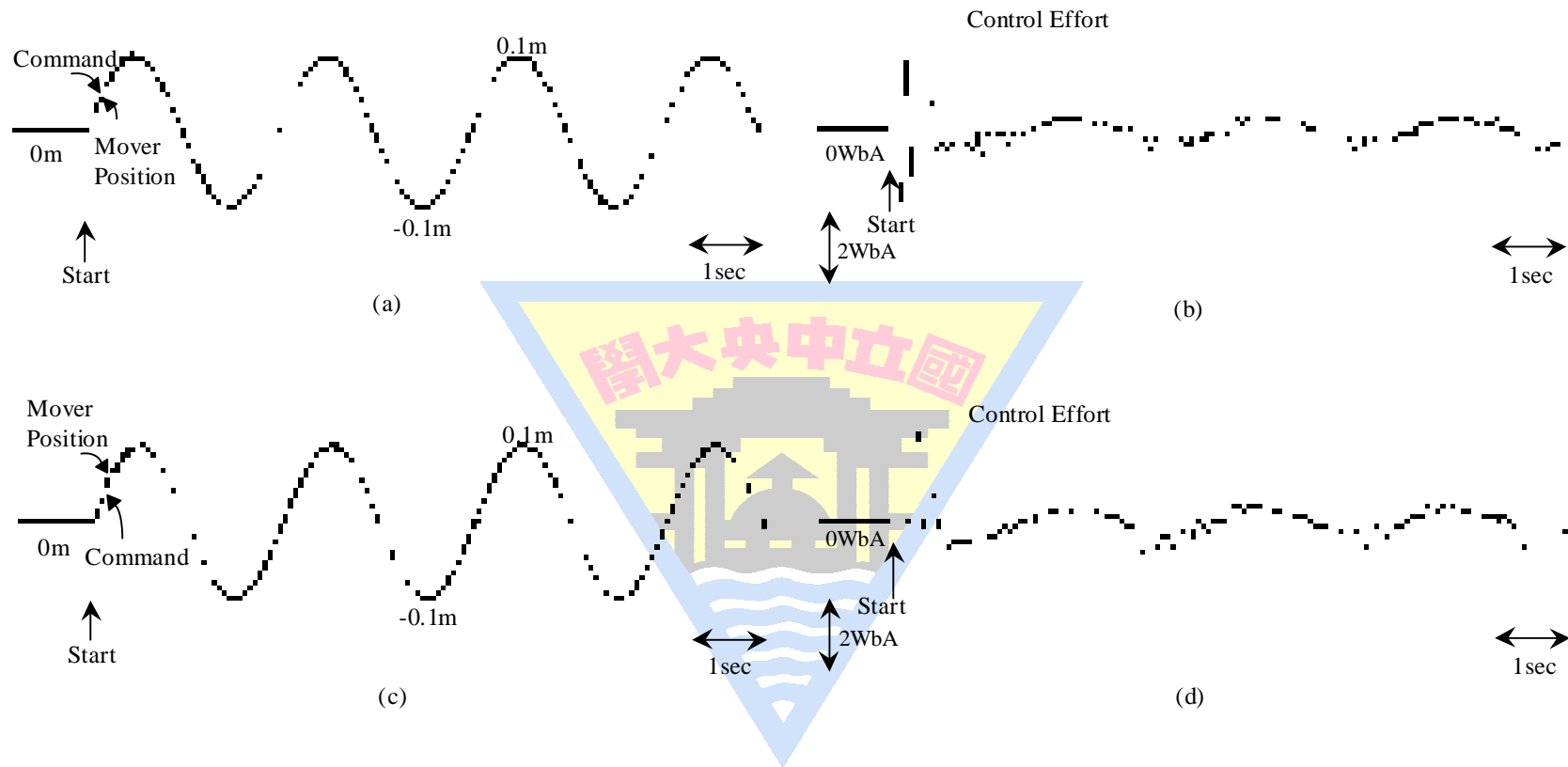


Fig. 6

II. Linear Synchronous Motor Drive

- Direct drive design of mechanical applications based on LSM is a viable candidate to meet the ever increasing demands for higher contouring accuracy at high machine speeds due to the following advantages over its indirect counterpart: 1. no backlash and less friction; 2. high speed and high precision in long distance location, i.e., the velocity is only limited by the encoder bandwidth or by the power electronics; 3. simple mechanical construction, resulting in higher reliability and frame stiffness; 4. high thrust force. The LSM is suitable for high-performance servo applications and has been used widely for the industrial robots, semiconductor manufacturing systems, and machine tools, etc.

- LSM is greatly affected by torque ripple, parameter variations and external load disturbances in the servo drive system because it is not equipped with auxiliary mechanisms such as gears or ball screws.
- To compensate these equivalent force disturbances, which directly impose on the mover of the PMLSM, quickly is very important. In order to achieve accurate tracking in high-performance position control system sophisticated control strategy is often required.
- An experimental PMLSM is shown in Fig. 7. The electromagnetic thrust force is produced by the interaction between secondary NdFeB magnet and magnetic field of AC windings included in the mover.

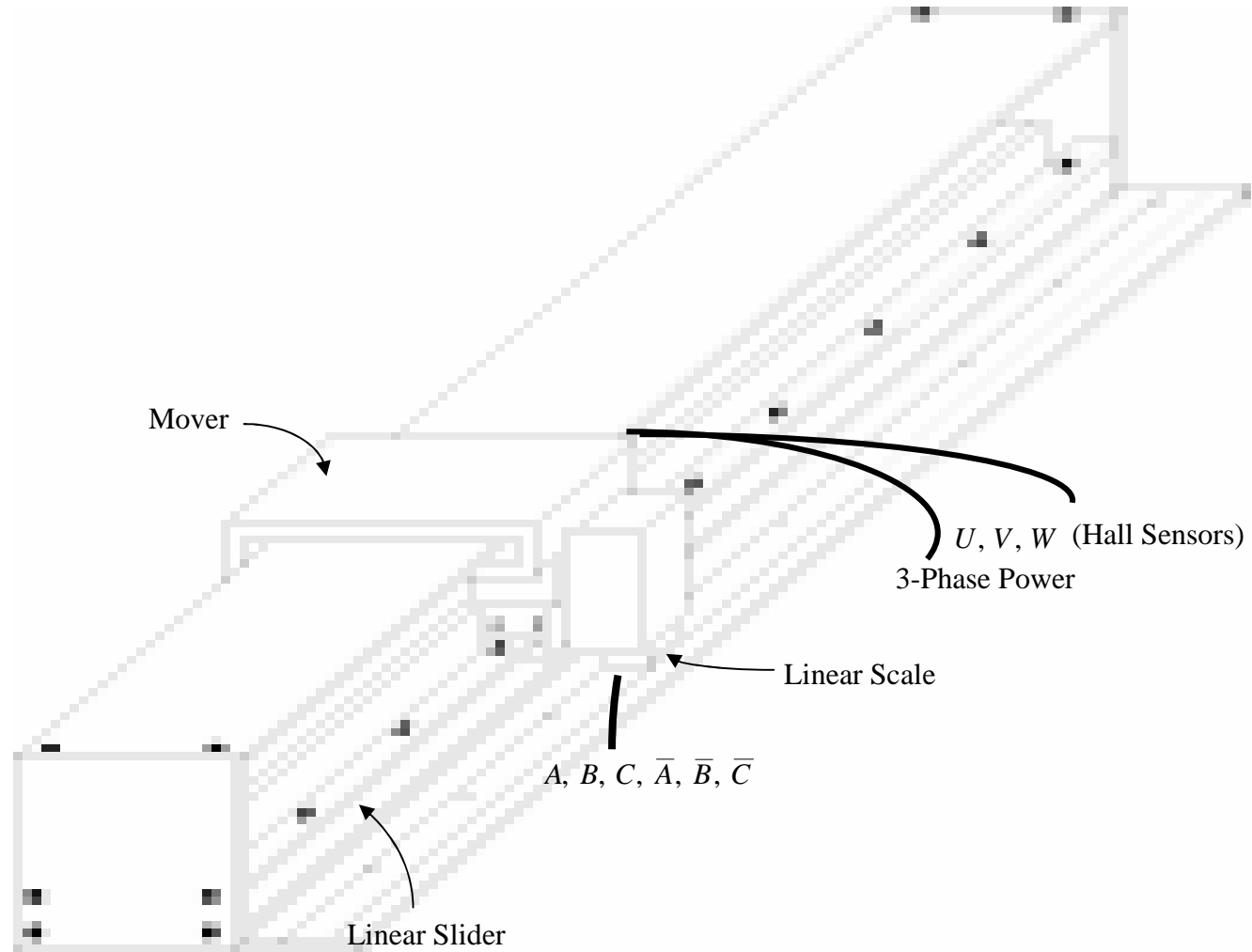


Fig. 7

-
- The configuration of a field-oriented PMLSM servo drive system is shown in Fig. 8.



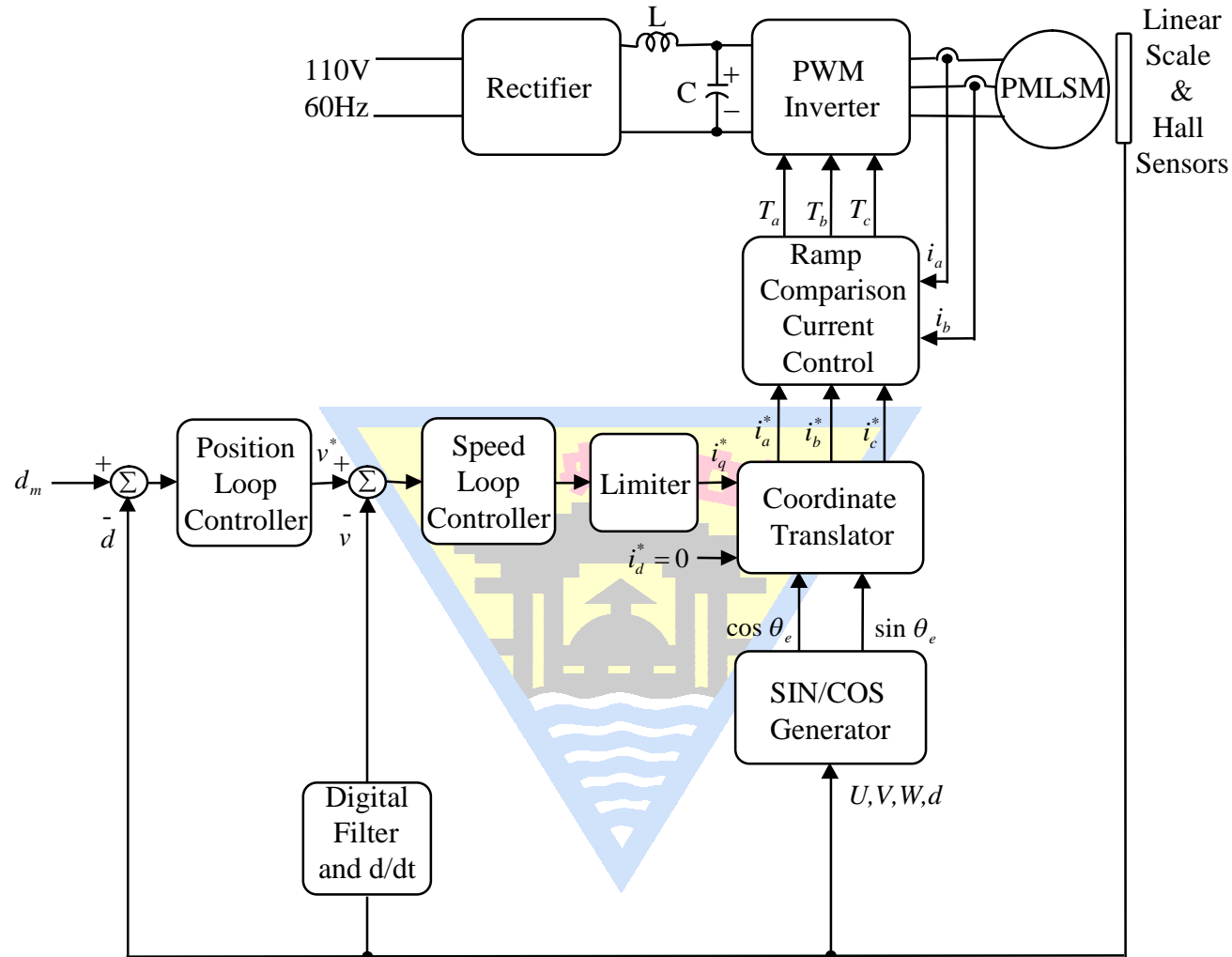


Fig. 8

- Machine model of a PMLSM described in synchronous rotating reference frame:

$$v_q = R_s i_q + p \lambda_q + \omega_e \lambda_d \quad (1)$$

$$v_d = R_s i_d + p \lambda_d - \omega_e \lambda_q \quad (2)$$

where

$$\lambda_q = L_q i_q \quad (3)$$

$$\lambda_d = L_d i_d + \lambda_{PM} \quad (4)$$

$$\omega_e = n_p \omega_r \quad (5)$$

and

$$\omega_r = \pi v / \tau \quad (6)$$

$$v_e = n_p v = 2\tau f_e \quad (7)$$

v is the linear velocity; τ is the linear velocity; v_e is the linear velocity.



- The electromagnetic force is

$$F_e = 3\pi n_p [\lambda_d i_q + (L_d - L_q) i_d i_q] / 2\tau \quad (9)$$

- The mover dynamic equation is

$$F_e = Mpv + Dv + F_L \quad (10)$$

- The basic control approach of a PMLSM servo drive is based on field orientation. The maximum force per ampere can be achieved. The resulted force equation is

$$F_e = 3\pi \lambda_{PM} i_q / 2\tau \quad (11)$$

- A hybrid supervisory control system shown in Fig. 9 is proposed to control the mover of the PMLSM for periodic motion. The supervisory control law is designed based on the uncertainty bounds of the controlled system to stabilize the system states around a predefined bound region. Since the supervisory control law will induce excessive and chattering control effort, the intelligent control system is introduced to smooth and reduce the control effort when the system states are inside the predefined bound region.

- In the intelligent control system, the RFNN control is the main tracking controller which is used to mimic a idea control law, and a compensated control is proposed to compensate the difference between the idea control law and the RFNN control.
- A four-layer RFNN as shown in Fig. 10, which comprises the input (the i layer), membership (the j layer), rule (the k layer) and output layer (the o layer), is adopted to implement the RFNN controller in this study.

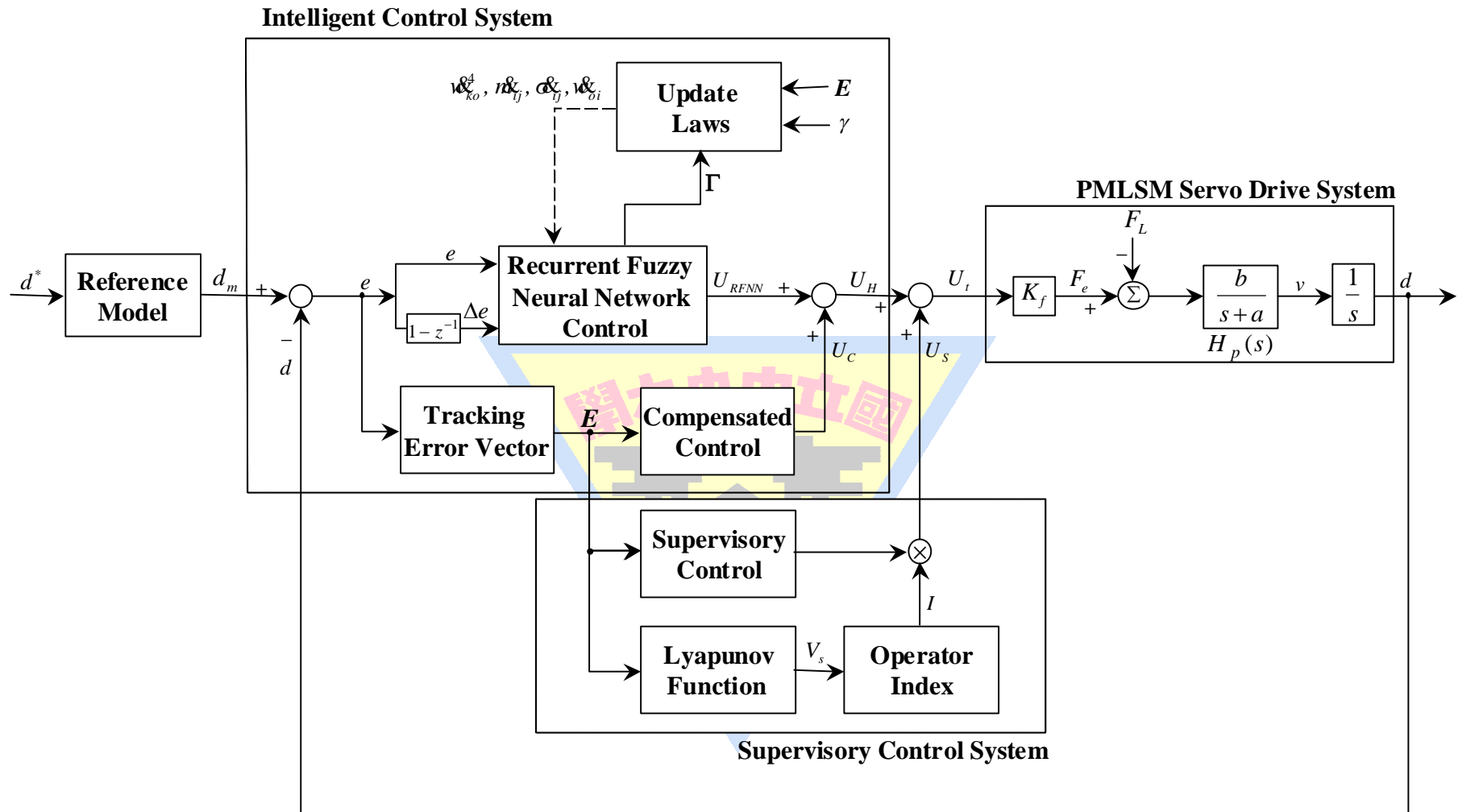


Fig. 9

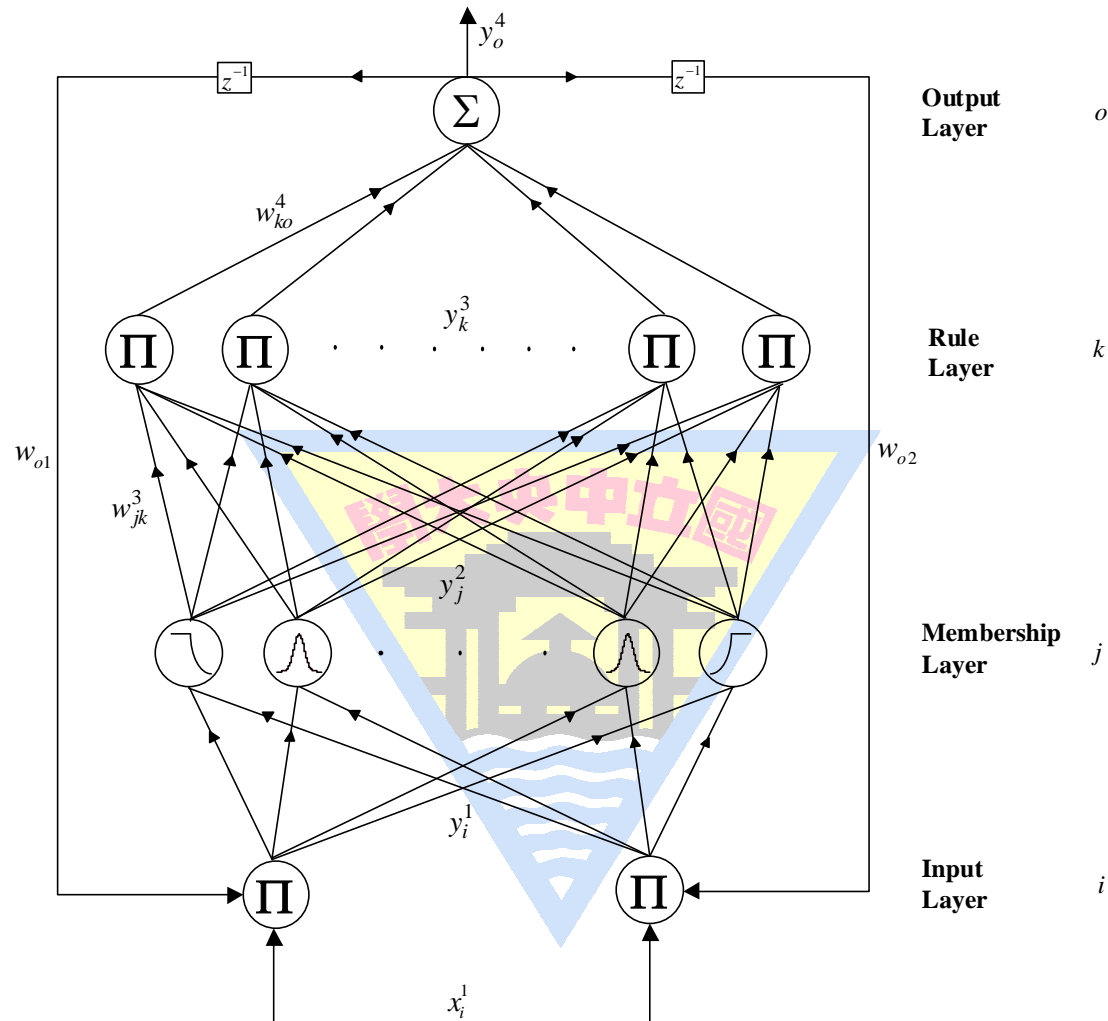
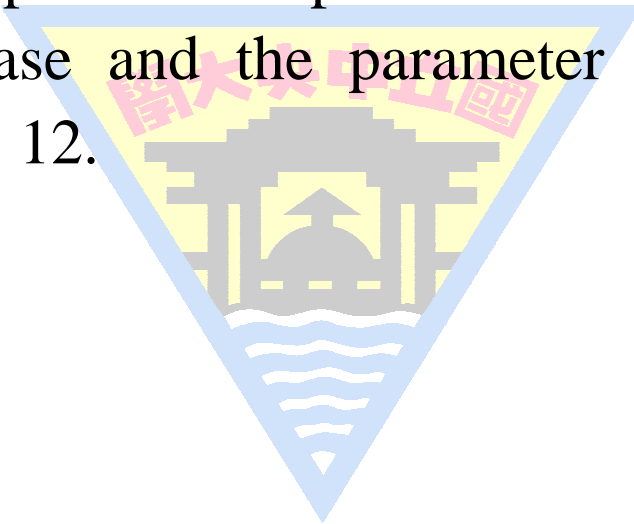


Fig. 10

- The block diagram of the computer control system for the field-oriented PMLSM servo drive is shown in Fig. 11.
- Experimental results of the hybrid supervisory control system due to periodic step and sinusoidal commands at the nominal case and the parameter variation case are depicted in Fig. 12.



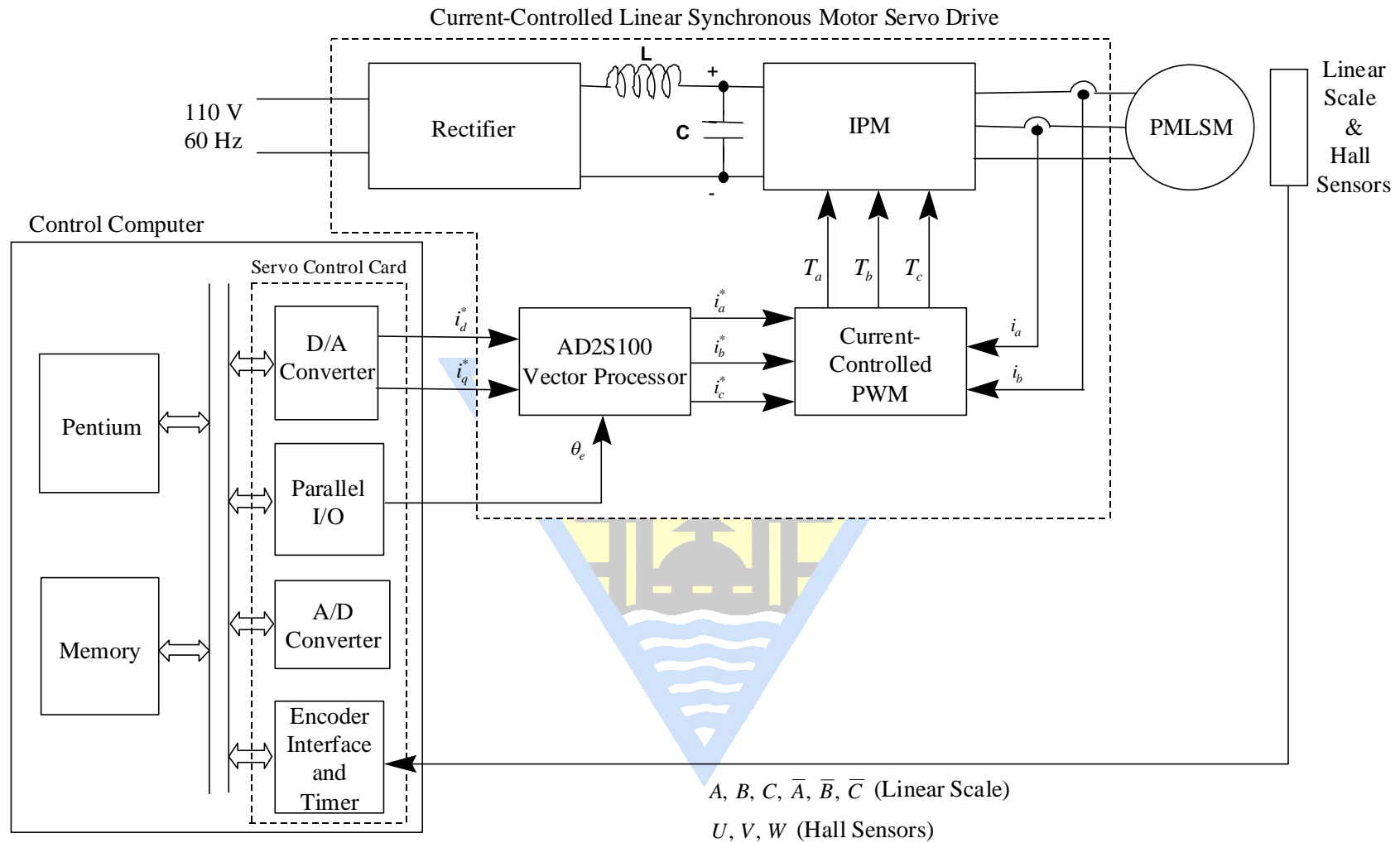


Fig. 11

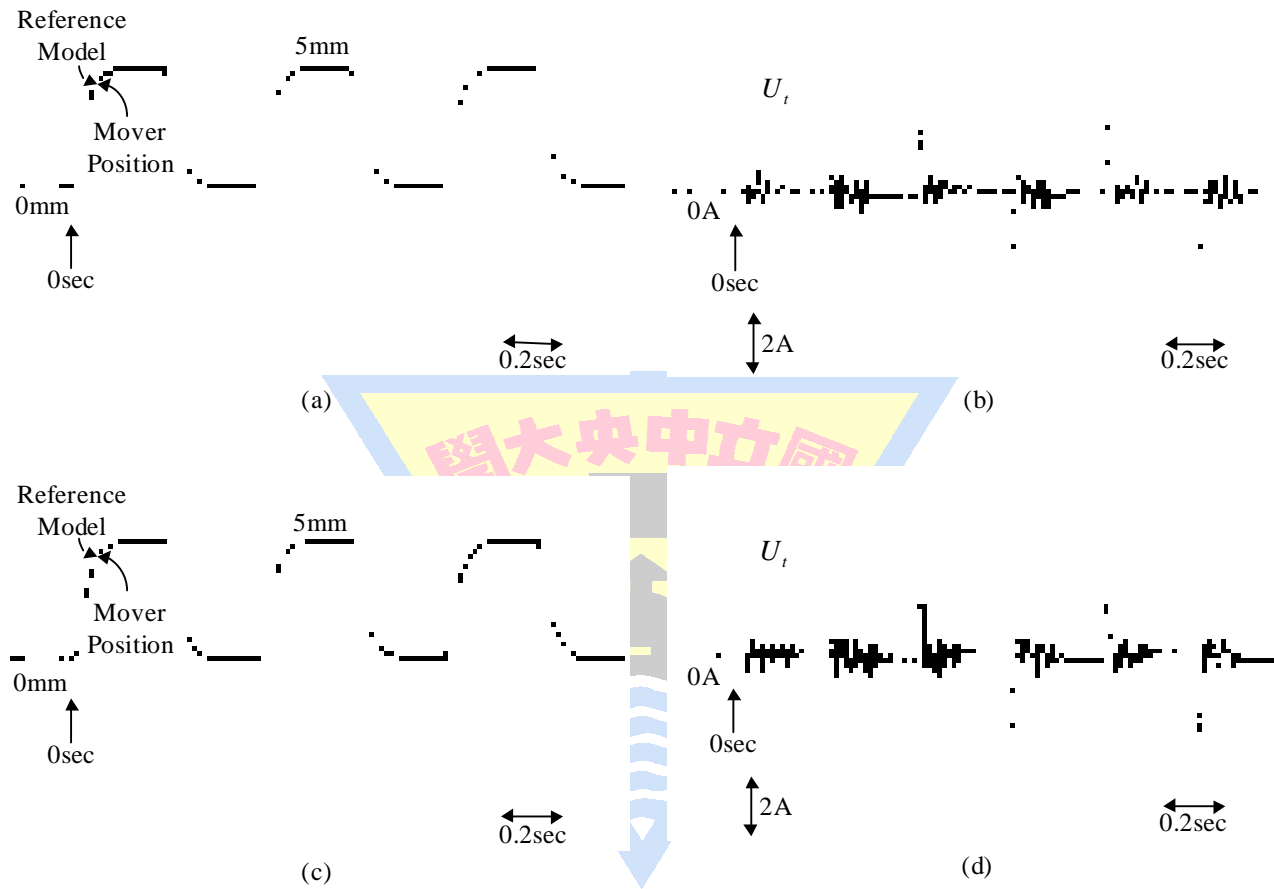


Fig. 12

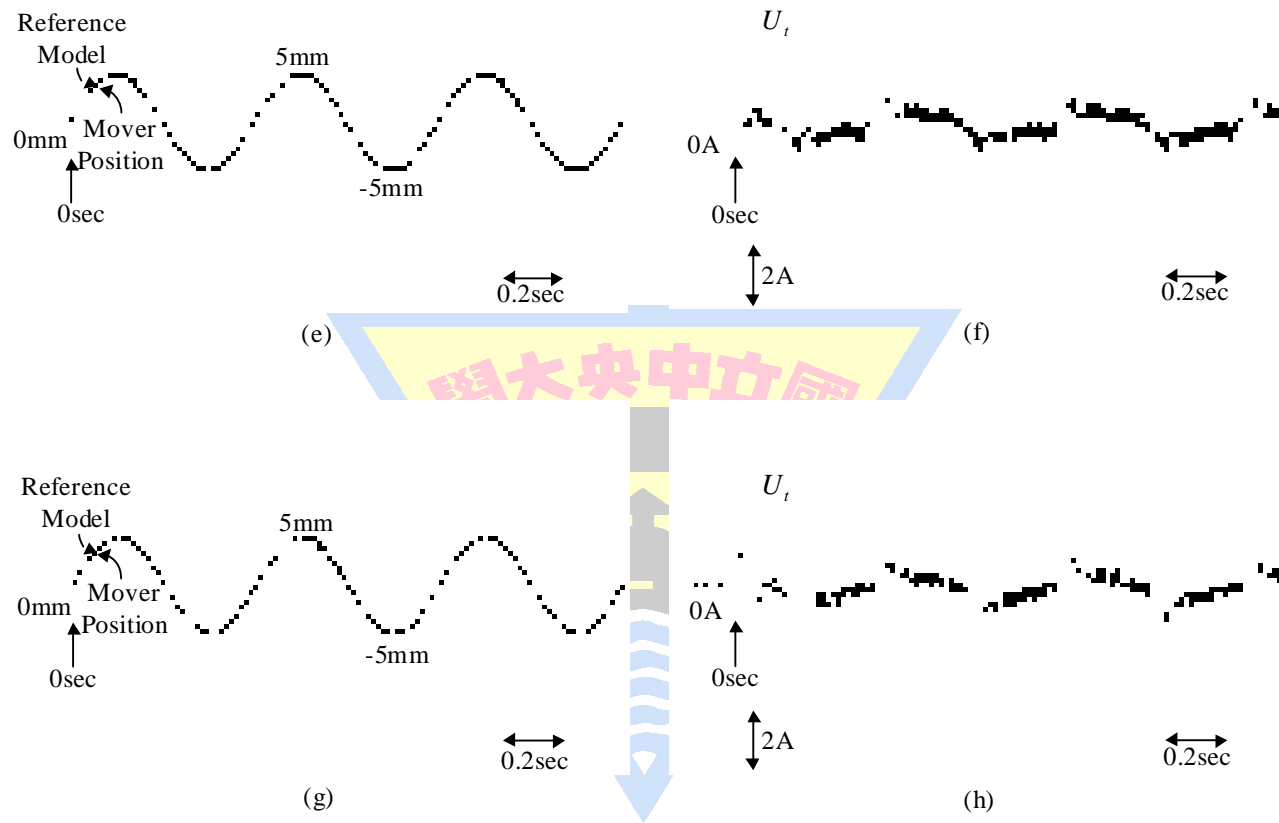


Fig. 12 (Cont.)

III. Piezo Ceramic Linear Ultrasonic Motor Drive

- Piezoelectric ceramic linear ultrasonic motors (LUSMs) are one of the new kinds of USMs. Different constructions and driving principles of LUSMs have been reported. They permit high precision, fast control dynamics and large driving force in small dimensions.
- SP series piezoelectric ceramic LUSMs of Nanomotion Ltd. have 1 micrometer of motion accuracy in open loop operation and 50 nanometers in closed loop operation. Control accuracy is much influenced by the existence of uncertainties, which usually comprises parameter variations, external disturbances and high-order dynamics, etc.

- The SP series piezoelectric motor shown in Fig. 13 comprises a thin rectangular piezoelectric ceramic having four electrodes on the front face and one electrode grounded on the rear face. These motors are operated using the double-mode vibrations under suitable excitation. To generate the different moving direction, the electrodes are electrified using an AC voltage in the pair of the diagonal electrodes.

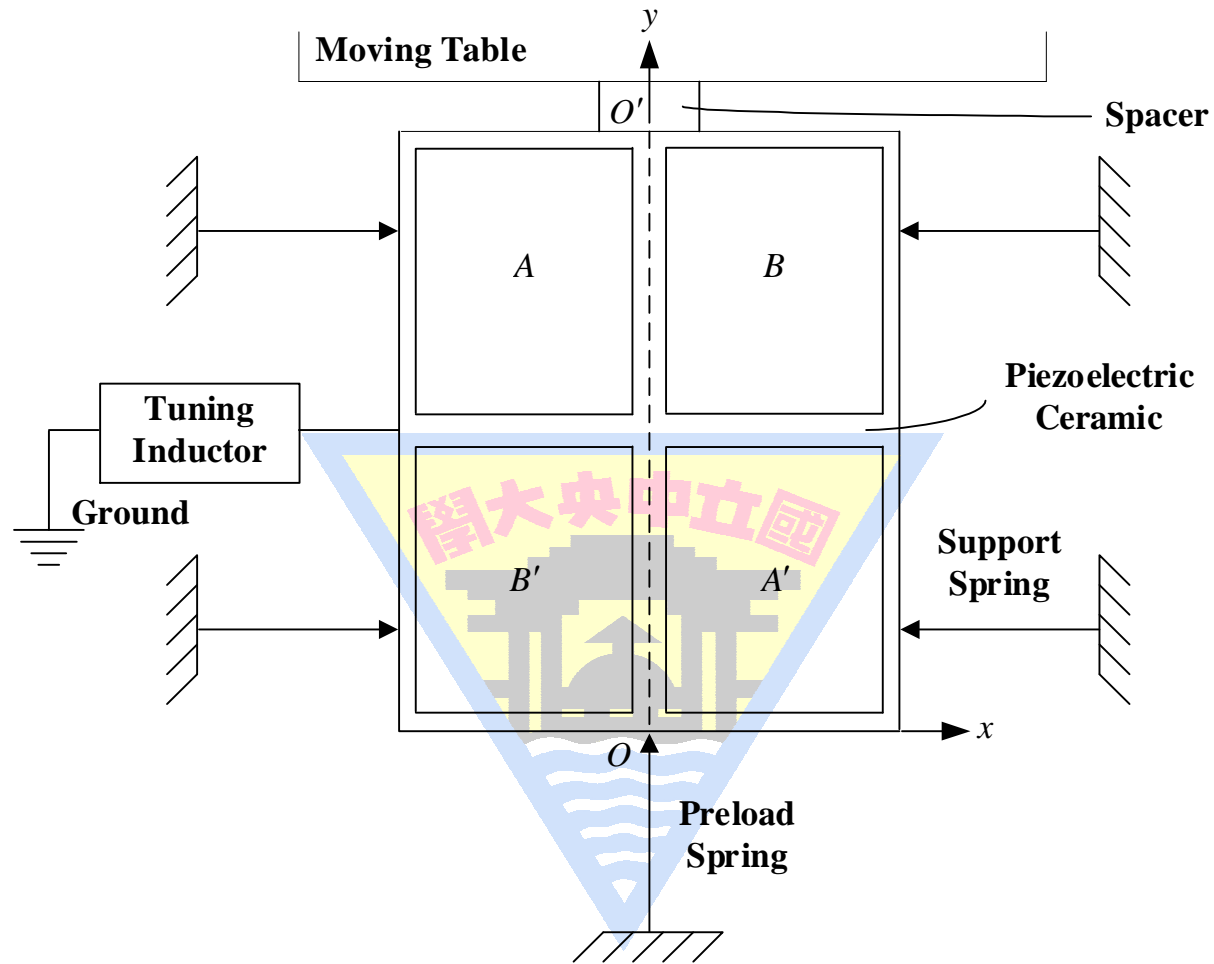


Fig. 13

- The dynamic characteristics of the LUSM are nonlinear and precise dynamic model is difficult to obtain, moreover, the motor parameters are time varying. A RFNN control system shown in Fig. 14 is proposed to control the position of the moving table of the LUSM to achieve high precision positioning with robust control characteristics. To guarantee the convergence of tracking errors, analytical methods based on a discrete-type Lyapunov function are proposed to determine the varied learning rates of the RFNN.

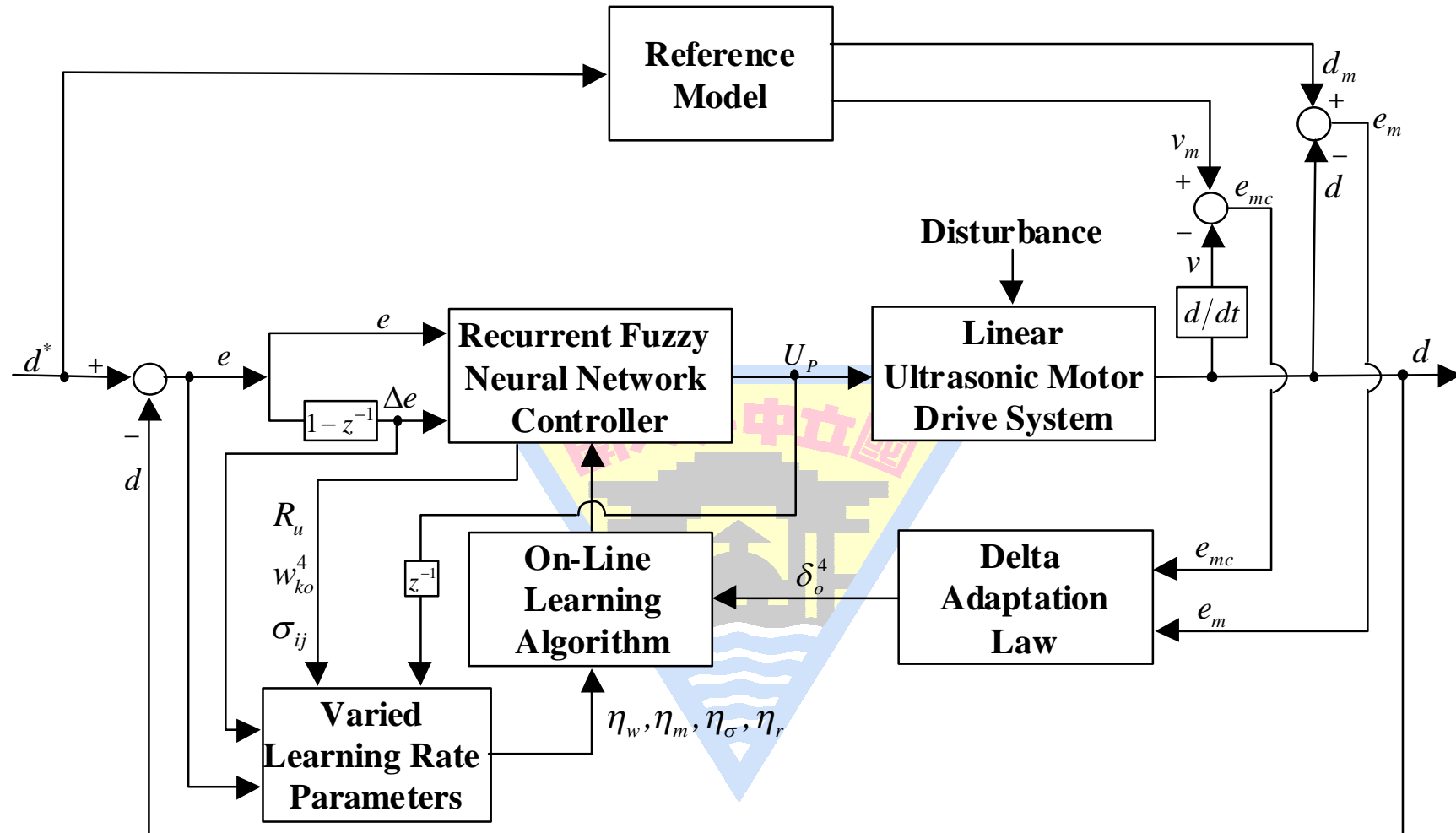


Fig. 14

- Block diagram of the computer control system for the LUSM drive is depicted in Fig. 15. The adopted LUSM is a 5W 240Vrms 70mA rms type and dynamic stall force 4N.
- LUSM is driven using a full-bridge voltage source inverter based on unipolar switching technique, in which the output of the RFNN is used as the control voltage of PWM. The inverter comprises a full-bridge DC-DC converter and in series with a *LC* resonant tank. The output of the *LC* resonant tank is a high voltage sinusoidal wave at the same frequency (39.6kHz), and the amplitude is proportional to the duty cycle of the PWM square wave.

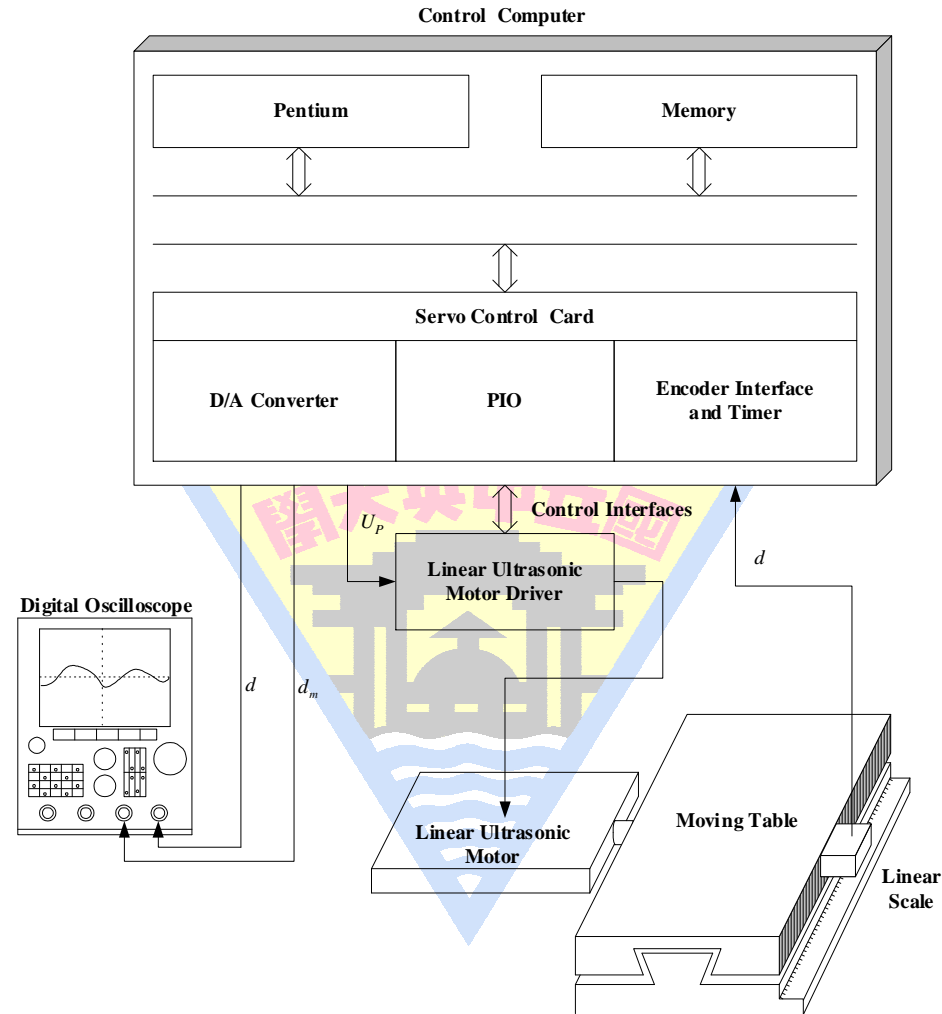


Fig. 15

- Experimental results of the proposed RFNN control system at the nominal case and the parameter variation case due to periodic step and sinusoidal commands are depicted in Figs. 16 and 17.



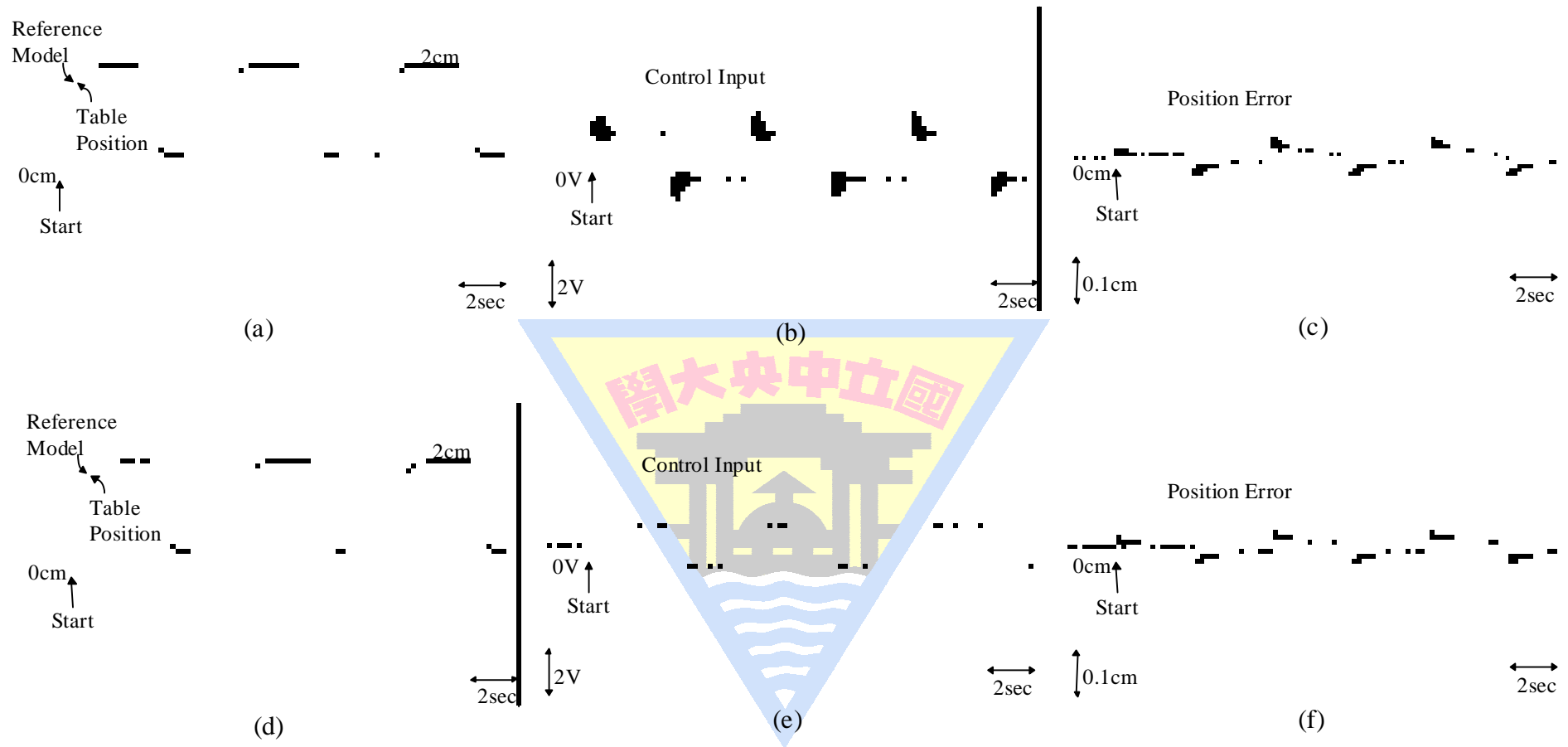


Fig. 16

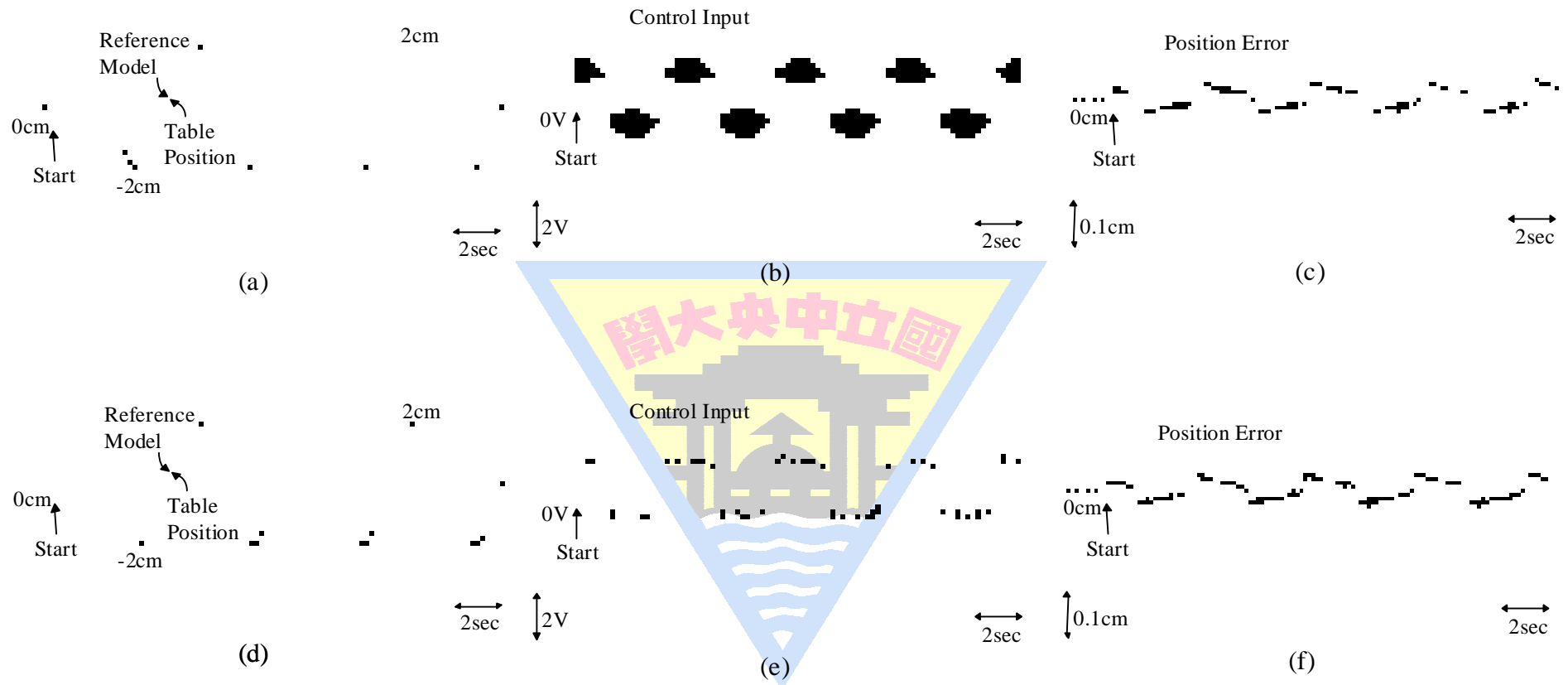


Fig. 17



IV. X-Y Table Based on Permanent Magnet Linear Synchronous Motor (PMLSM)

- In modern manufacturing, the design of the two-axis motion control with high-performance and high-precision machining is substantially required.
- The motion control of an X-Y table, which is composed of two PMLSMs, is considered. Such a system can be found in many applications, e.g., machine tools and integrated circuit (IC) manufacturing equipment.
- The PMLSM is suitable for high-performance servo applications and has been used widely for the industrial robots, machine tools, semiconductor manufacturing systems, and X-Y driving devices, etc.

- Since the operation of PMLSM involves two contacting bodies, nonlinear friction force is inevitably among the forces of motion. The friction characteristic may be easily varied due to the change of normal forces in contact, temperature and humidity.
- Friction is a natural phenomenon that is quite difficult to model, and it is not completely understood. Therefore, the precise friction model is impossible to obtain in practical applications.
- To obtain high-performance motion control system, the compensation of the uncertainties and nonlinear friction force, which directly impose on the mover of the PMLSM, quickly and directly is very important.

- Floating-point DSPs offer all advantages of conventional DSPs in combination with precise floating-point arithmetic.
- With on-board analog-to-digital converters (ADCs), digital-to-analog converters (DACs), parallel input/output (PIO) and encoder interface, the adopted board has greatly simplified the task of implementing digital controllers using desktop computers.
- The X-Y table machine used is composed of two PMLSMs which includes a long stationary tubular “secondary” with guidance rail and linear scale, and a moving short “primary” which contains the core armature winding and Hall sensing elements as shown in Fig. 18.

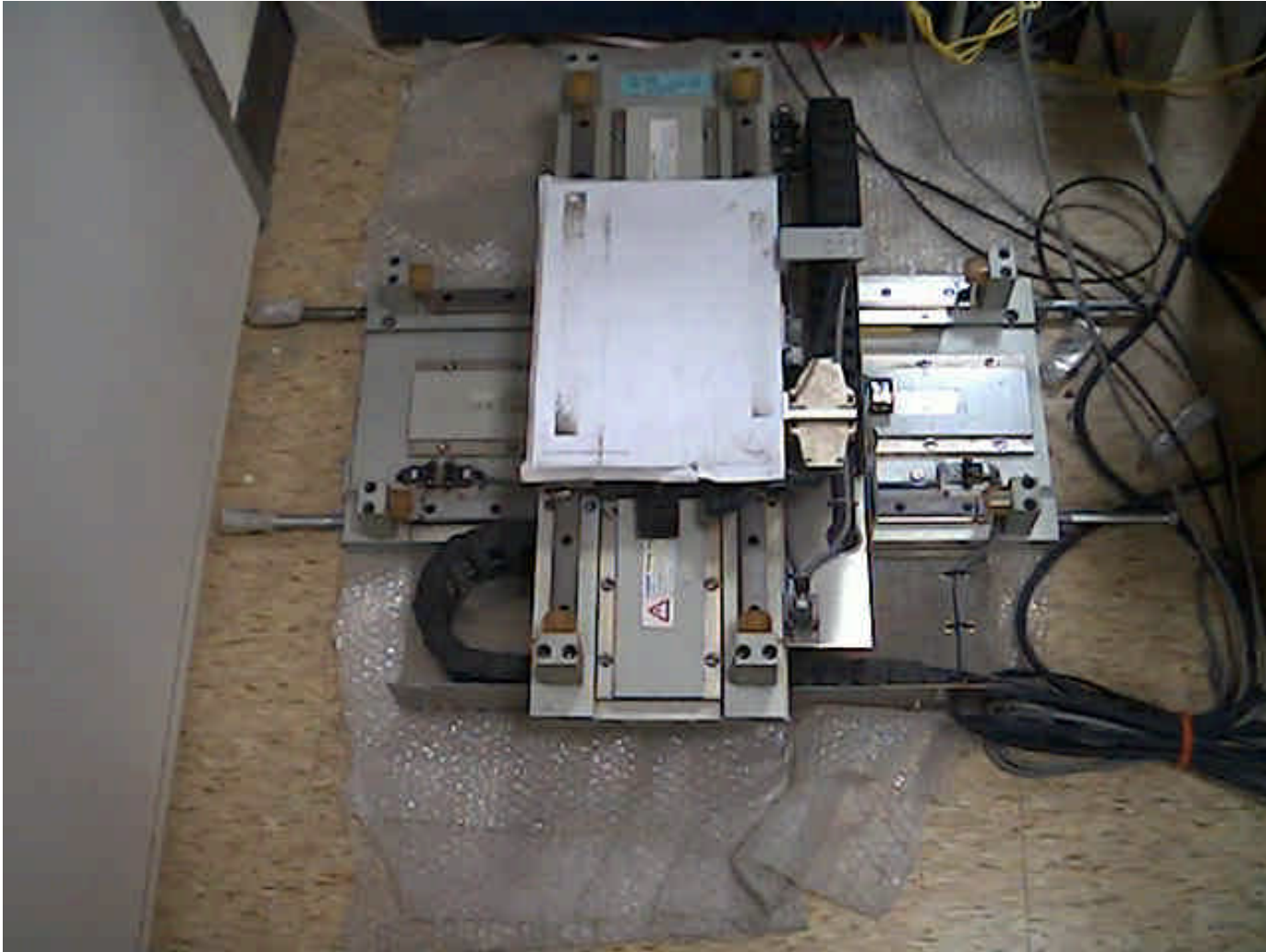


Fig. 18

- With the implementation of the field-oriented control, the electromagnetic force can be simplified as follows:

$$F_{ei} = K_{fi} i_{qi}^* \quad (1)$$

$$K_{fi} = 3 \pi n_{pi} \lambda_{PMi} / (2\tau_i) \quad (2)$$

where $i = x, y$ (x and y denote the axis); K_{fi} is the thrust coefficient; i_{qi}^* is the thrust current command.

- The mover dynamic equation is

$$F_{ei} = M_i \dot{v}_i + D_i v_i + F_{Li} + f_i(v) \quad (3)$$

- Considering Coulomb friction, viscous friction and Stribeck effect, the nonlinear friction force can be formulated as follows:

$$f_i(v) = F_{Ci} \text{sgn}(v_i) + (F_{Si} - F_{Ci}) e^{-(v_i/v_{si})^2} \text{sgn}(v_i) + K_{vi} v_i \quad (4)$$

where F_{Ci} is the Coulomb friction;

F_{Si} is the static friction;

v_{si} is the Stribeck velocity parameter;

K_{vi} is the coefficient of viscous friction;

$\text{sgn}(\cdot)$ is a sign function.

- The configuration of the proposed robust fuzzy-neural-network (RFNN) sliding-mode control system for a single-axis PMLSM is depicted in Fig. 19.
- In the proposed RFNN sliding-mode control system, an FNN with accurate approximation capability is employed to approximate a nonlinear function including the lumped uncertainty of the X-Y table. Moreover, a robust controller is proposed to confront the minimum approximation error and high-order terms in Taylor series. Furthermore, the adaptive learning algorithms in the RFNN sliding-mode control system are derived using the Lyapunov stability analysis, so that system-tracking stability can be guaranteed in the closed-loop system.

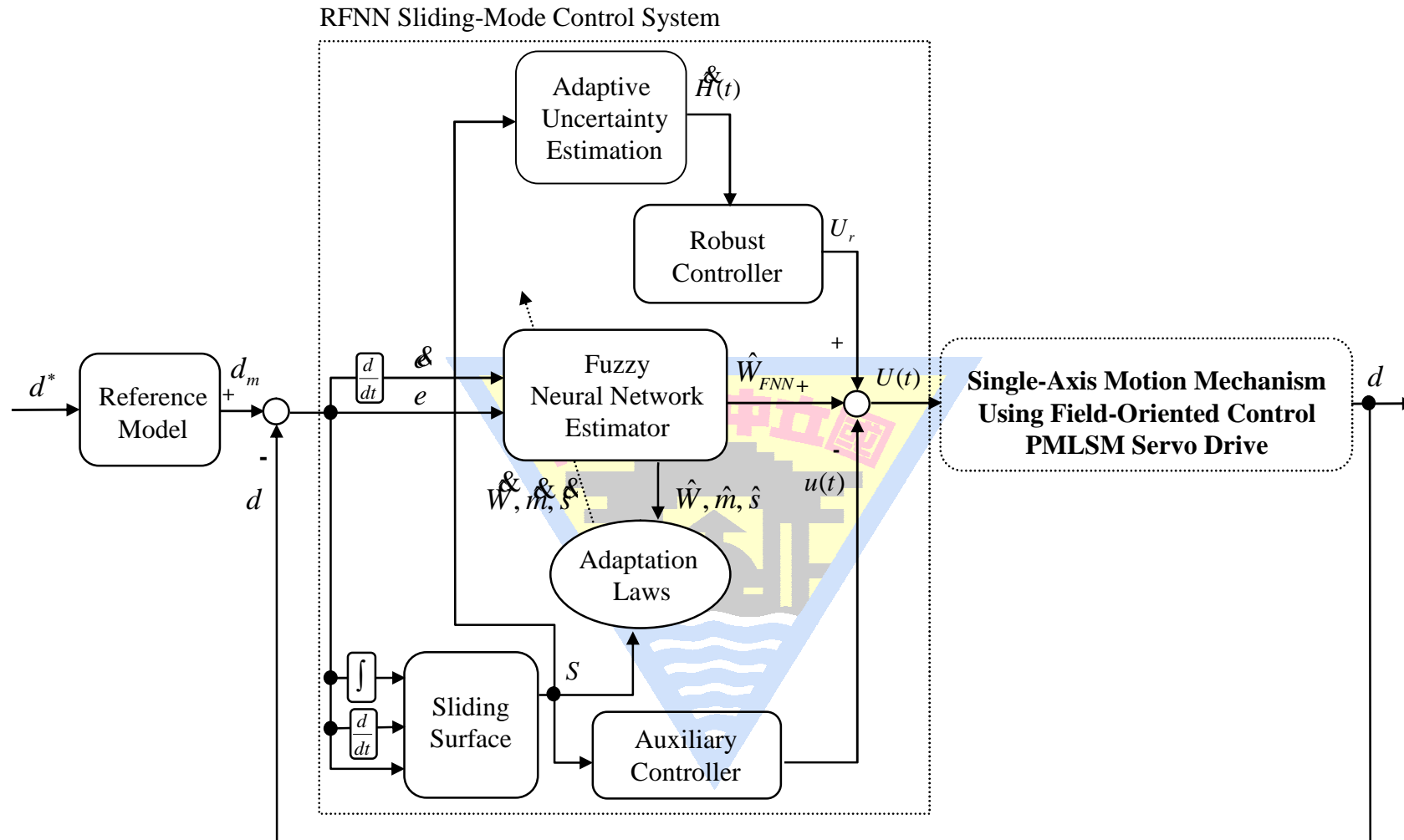


Fig. 19

- A four-layer FNN which comprising an input, a membership, a rule and an output layer, is adopted to implement the proposed FNN controller. It can be represented in the following form:

$$y = W_{FNN}(\mathbf{r}, \Theta, \mathbf{m}, s) \equiv \Theta \Gamma \quad (5)$$

where

$\Theta \in R^{1 \times k}$ is the adjustable weights vector in the rule-to-output layer ;

$\Gamma = \Gamma(\mathbf{Q}) = \mu \mathbf{Q}(\mathbf{r}) \in R^{k \times 1}$ is the output vector of membership layer ;

$\mathbf{r} = [e(t) \quad \dot{e}(t)] \in R^{2 \times 1}$ is the input state of FNN ;

$\mathbf{Q}(\mathbf{r}) = \exp\left\{-\frac{[(\mathbf{a}\mathbf{r}) - \mathbf{m}]^2}{s^2}\right\} \in R^{j \times 1}$ is the membership function used in the FNN ;

in which $\mathbf{m} \in R^{j \times 1}$ and $s \in R^{j \times 1}$ are the adjustable parameter vectors of means and standard deviations of the Gaussian functions.

- A control methodology is proposed to guarantee the closed-loop stability and perfect tracking performance and to tune the means and standard deviations of FNN on line. To achieve this goal, a linearization technique using Taylor series is employed to transform the nonlinear FNN functions into partially linear form.
- If the adaptation laws of the FNN are designed as (6)~(8), then the stability of the controlled system can be guaranteed.

$$\dot{\hat{\Theta}} = \alpha_1 S(t) \hat{\Gamma}^T \quad (6)$$

$$\dot{m} = \alpha_2 \left(S(t) \hat{\Theta} \Gamma_m \right)^T \quad (7)$$

$$\dot{s} = \alpha_3 \left(S(t) \hat{\Theta} \Gamma_s \right)^T \quad (8)$$

where α_1 , α_2 and α_3 are positive constants; $S(t)$ is the sliding surface; Γ_m and Γ_s are the parameters of the expansion of Taylor series.

- The block diagram of the DSP-based computer control two-axis motion control system is shown in Fig. 20. A TMS320C32 floating-point DSP is the core of the control computer. Moreover, the control computer includes multi-channels of ADC, DAC, PIO and encoder interface. The current-controlled PWM VSI is implemented using an intelligent power module (IPM) switching component with a switching frequency of 15kHz. Digital filters and frequency multiplied by four circuits are built into the encoder interface circuits to increase the precision of position feedback. The resulted resolution is $1\ \mu\text{m}$.
- The field-oriented mechanism and the proposed RFNN sliding-mode control system are realized in the DSP using the “C” and “Assembly” language.

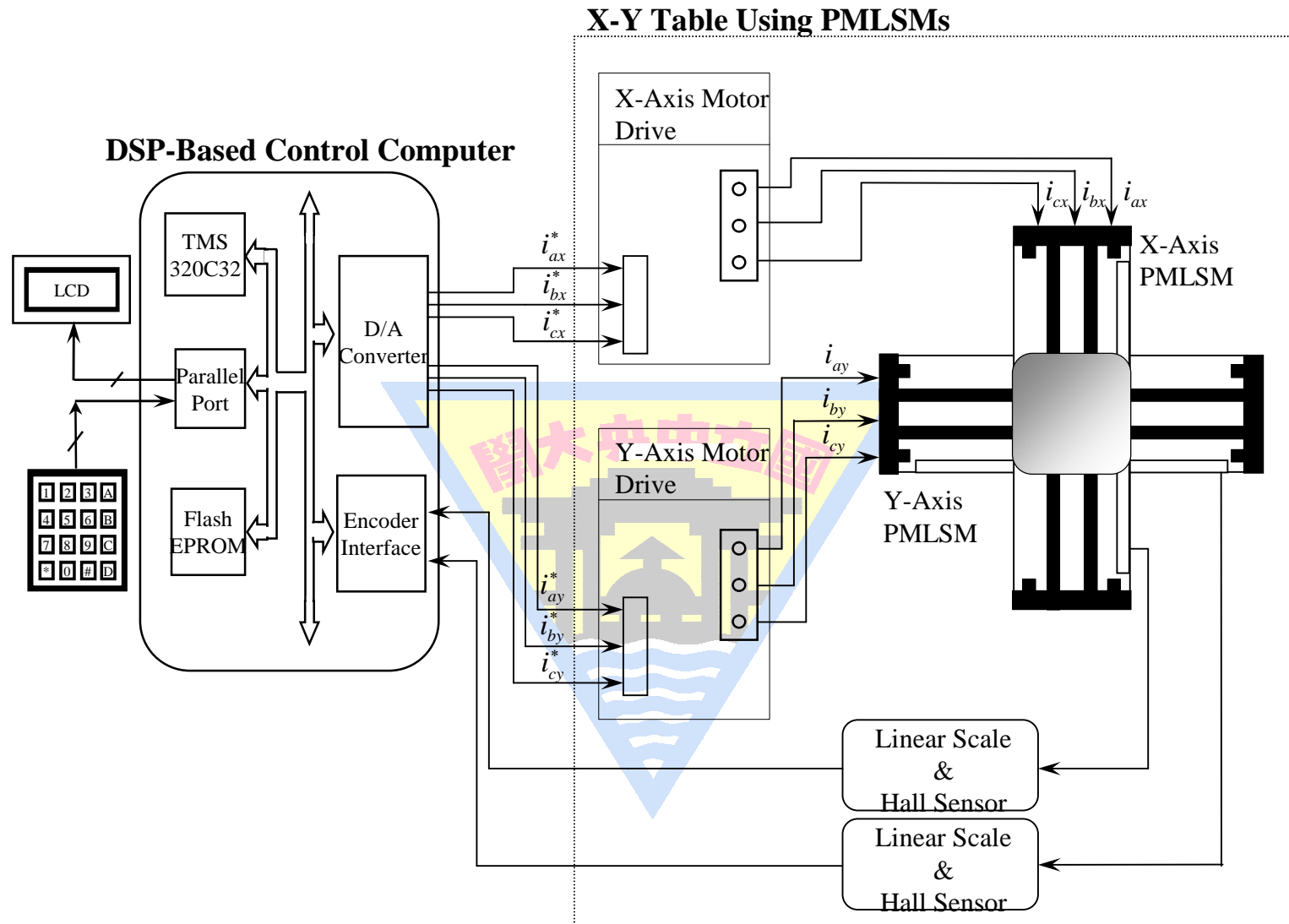


Fig. 20

- The methodology proposed for the implementation of the real-time RFNN sliding-mode control system are composed of main program, one interrupt service routine (ISR) and one subroutine “Control” in the DSP. In the main program, parameters and input/output (I/O) initialization are set first then the interrupt interval for the ISR is set. After enabling the interrupt, the ISR with 0.2ms sampling rate is used for the encoder interface and field-oriented mechanism.
- The ISR reads the mover position from the linear scale and Hall sensor and gets the control effort from the subroutine “Control” to calculate the three-phase current commands via field-oriented mechanism then sends the calculated three-phase current commands to the X-axis and Y-axis motor drives via DACs.

- Since the DSP control computer has only one hardware interrupt available, a parameter in the ISR is used to record the executing times of the ISR. When the parameter is equal to 5, the subroutine “Control” begins to execute so that it has 1.0ms sampling rate.
- The subroutine “Control” first reads the mover position from the encoder then calculates the motor velocity and the control effort according to the proposed RFNN sliding-mode control algorithm.

- The contour planning is very important to control the X-Y table effectively. Moreover, in practical applications the motion commands of X-axis and Y-axis are designed individually through contour planning to achieve two dimensions motion control.
- The circle, four leaves, star and window contours are adopted to show the control performance of the proposed RFNN sliding-mode control system.
- The reference contours are shown in Fig. 21.

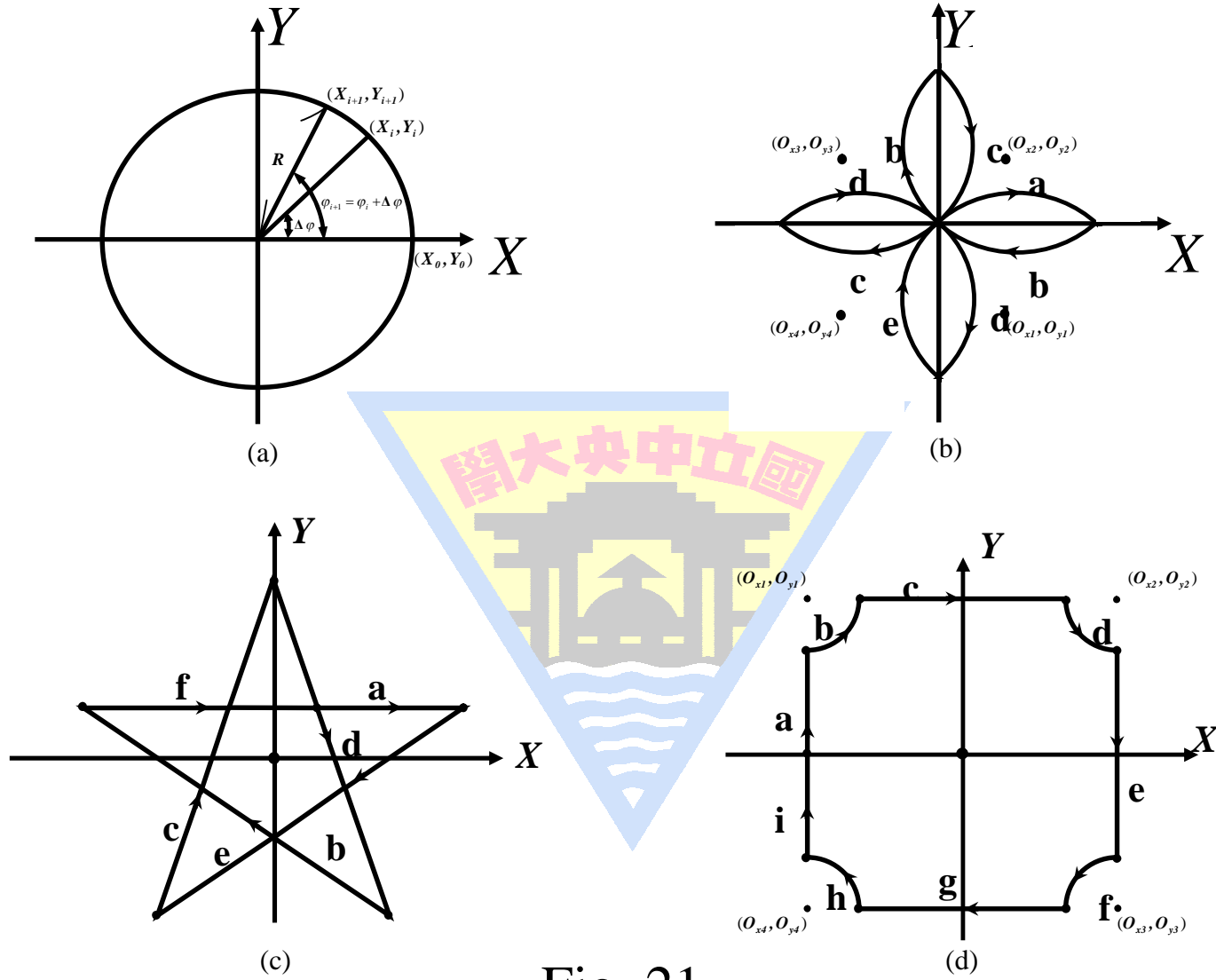


Fig. 21

- Experimental results of the tracking responses of the X-Y table, the control efforts and the tracking errors of the X-axis and Y-axis using the proposed RFNN sliding-mode control system due to circle and four leaves contours at the nominal condition are depicted in Figs. 22 and 23.
- Experimental results of the tracking response of the X-Y table, the control efforts and the tracking errors of the X-axis and Y-axis using the proposed RFNN sliding-mode control system due to circle and four leaves contours at the parameter variation condition are depicted in Figs. 24 and 25.

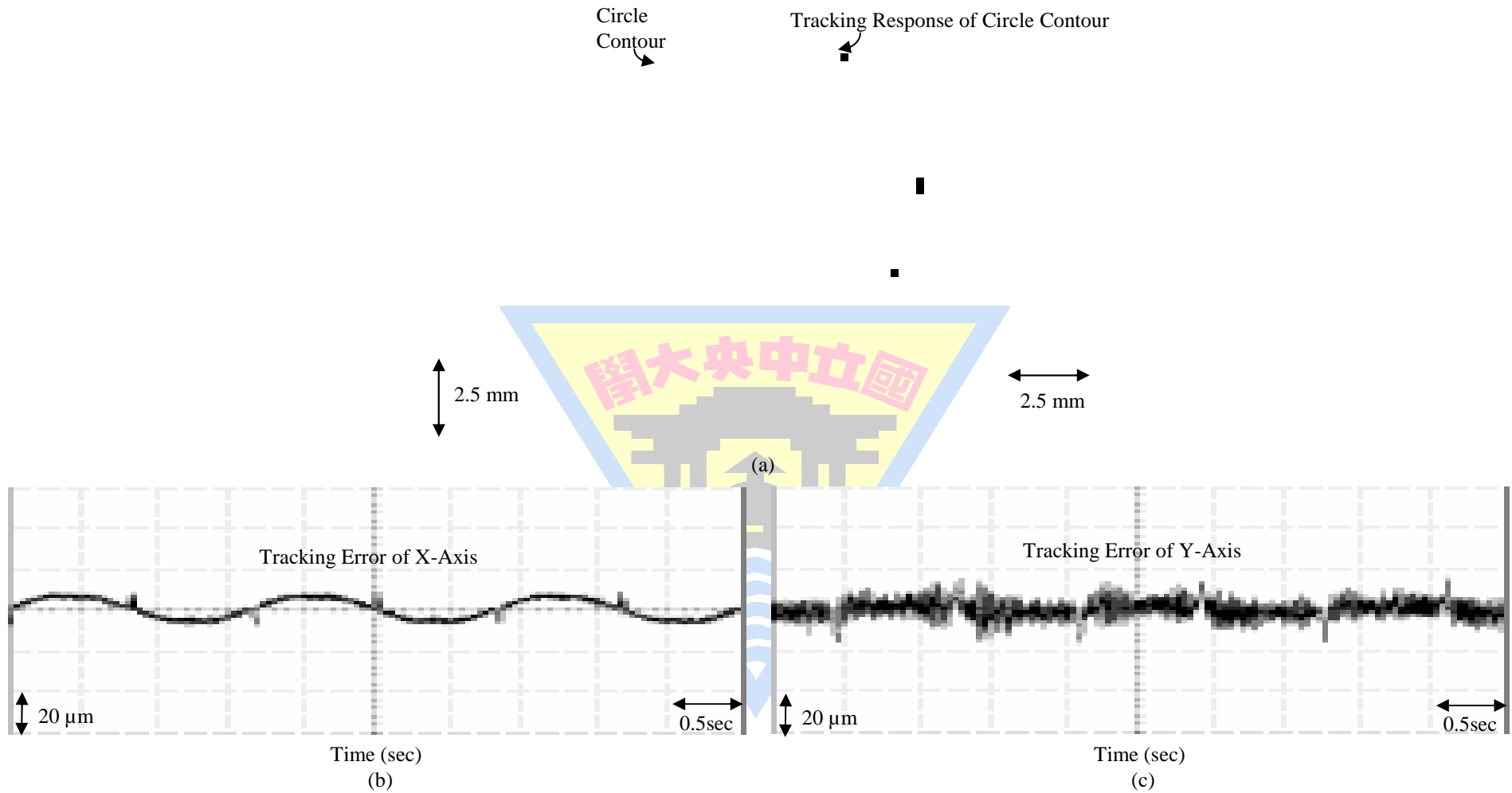


Fig. 22

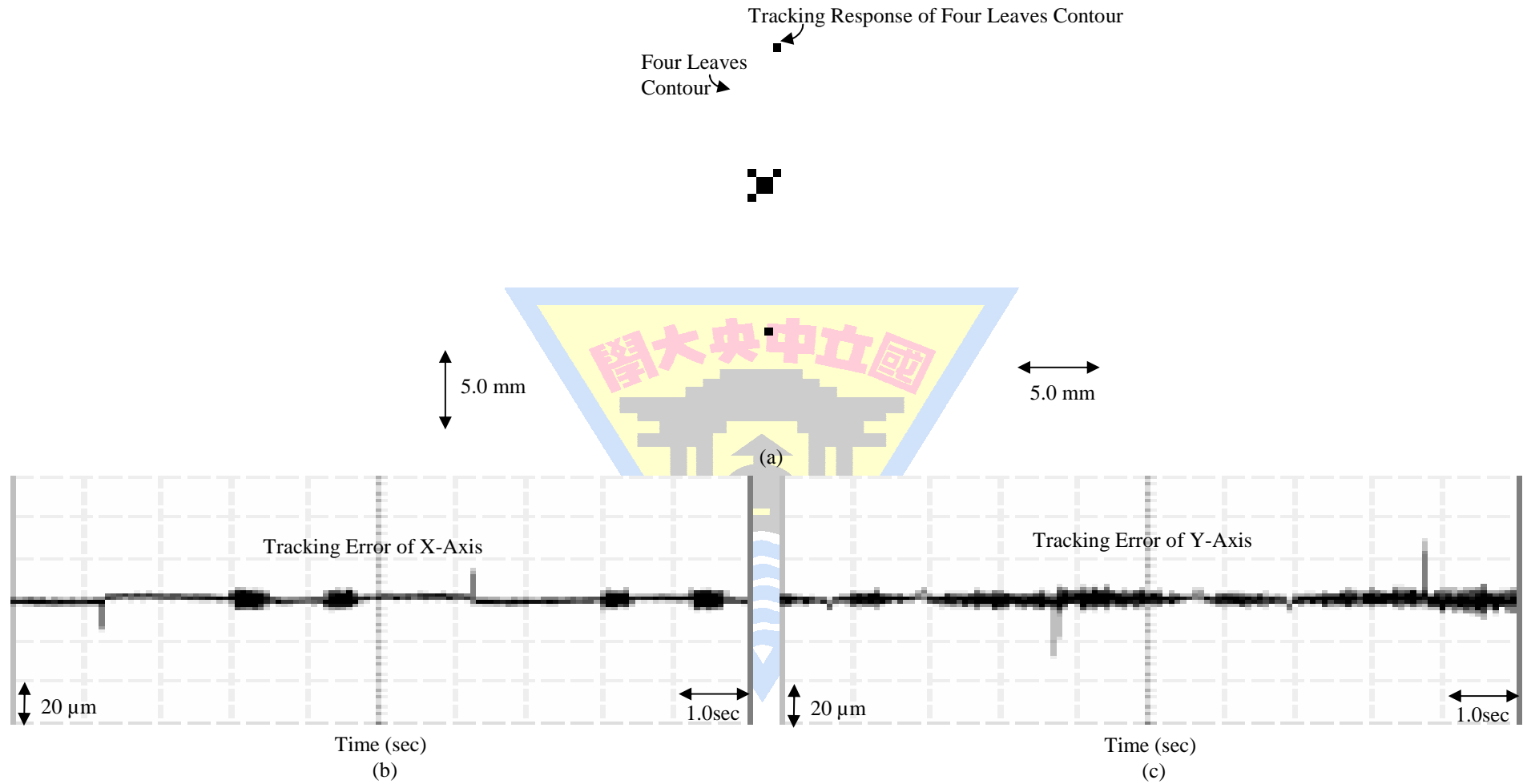


Fig. 23

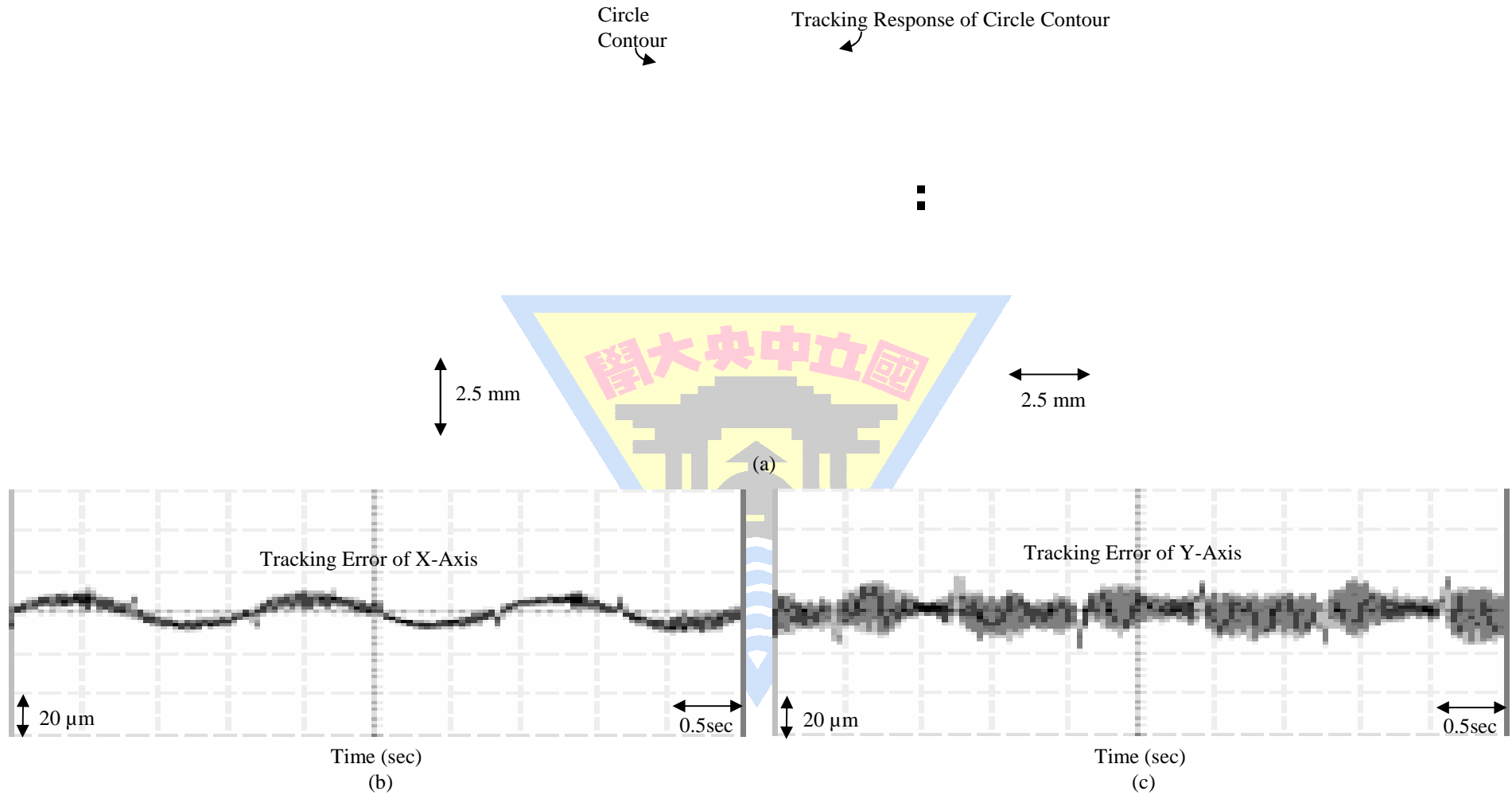


Fig. 24

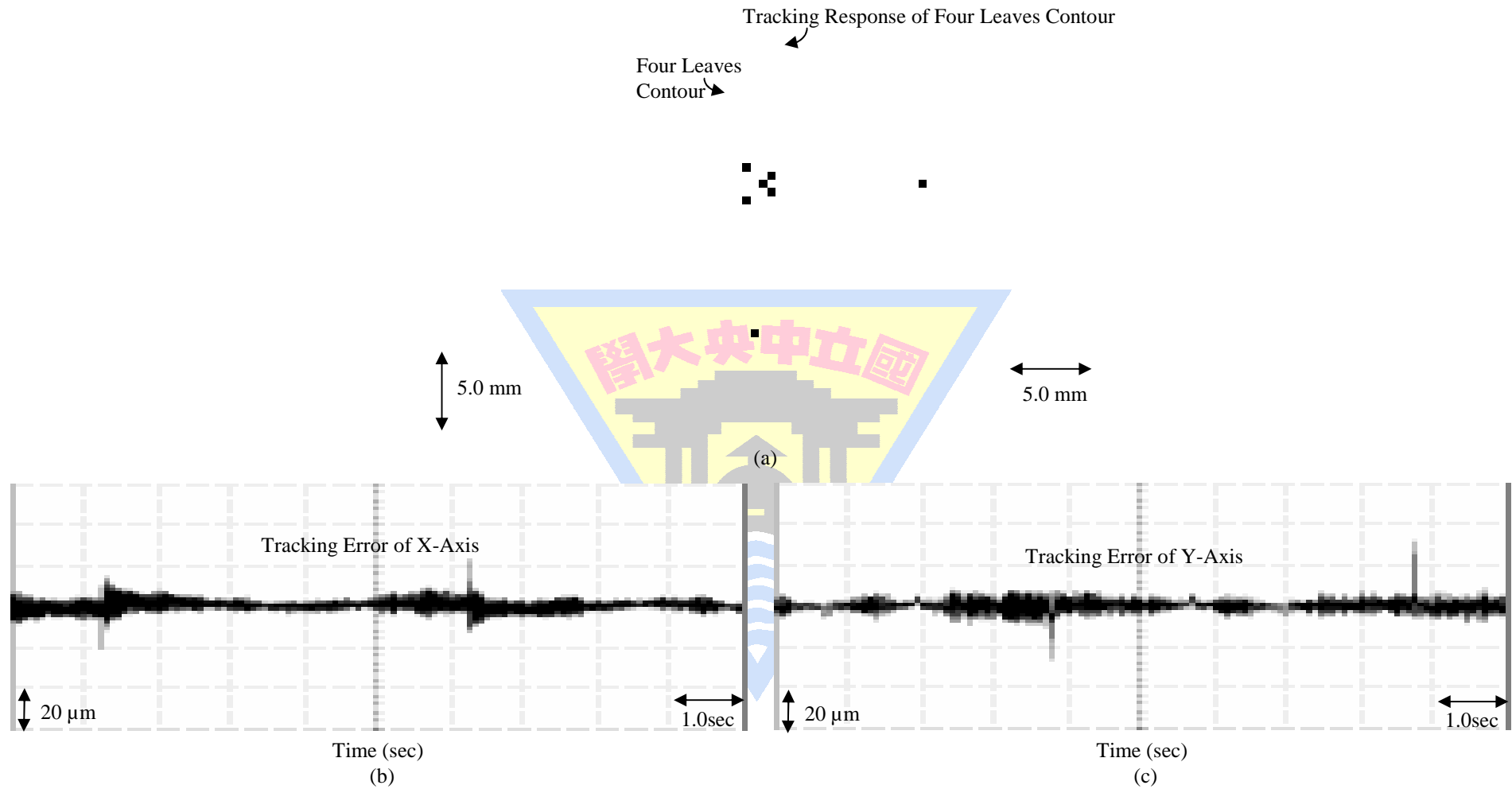


Fig. 25

V. Conclusions

- Selection of linear motor drives should be according to specific application.
- Feedback linearization and field-oriented control are implemented to decouple the force and flux of LIM and LSM.
- Current-controlled PWM VSI is implemented to drive LIM and LSM.
- Unipolar switching full-bridge PWM converter and *LC* resonant are implemented to drive the LUSM.

- The combination of linear/nonlinear and intelligent controllers is necessary for the LIM and LSM to achieve robust control performance.
- Intelligent controller is the only choice for the LUSM to achieve accuracy tracking response under the existence of uncertainties.
- For the convenience of graduated students, PC-based control system is adopted. In the future the control system should be implemented in DSP/FPGA or DSP/ASIC system.

**Thank You for Your
Attention!**